

Stroboscopic theory of atomic statistics in the micromaser

R.R. Puri*, S. Arun Kumar†, and R.K. Bullough‡

Department of Mathematics, UMIST, PO Box 88, Manchester M60 1QD, UK.

(October 29, 2018)

We study the statistics of the atoms emerging from the cavity of a micromaser in a dynamical, discrete-time ‘stroboscopic’ description which takes into account the measurements made, in general, with imperfect efficiencies $\eta < 1$, on the states of the outcoming atoms. Inverted atoms enter stochastically, in general, with a binomial distribution in discrete time; but we also consider the continuous-time limit of this input statistics which is Poissonian. We envisage two alternative experimental procedures: one of these is to consider a fixed number N of atoms pumped into the cavity and subsequently leaving it to undergo state detection; the other is to consider input of the excited atoms and their subsequent detection and collection in a fixed time t . We consider, in particular, the steady state behaviors achieved in the two limits, $N \rightarrow \infty$ and $t \rightarrow \infty$, as well as the approaches to these two limits. Although these limits are the same for the state of the cavity field, they are not the same, in general, for the observable outcoming atom statistics. We evaluate, in particular, Mandel’s Q -parameters Q_e (Q_g) for outcoming atoms detected in their excited states (ground states), for both $N \rightarrow \infty$ and $t \rightarrow \infty$, as functions of $N_{ex} = RT_c$: R is the mean rate of entry for the incoming atoms and T_c is the cavity damping time. The behavior of these atomic Q -parameters is compared with that parameter for the cavity field.

I. INTRODUCTION

The micromaser, in which two-level atoms enter a high- Q cavity one at a time and interact with a single mode of the cavity field before subsequently leaving the cavity, provides a valuable means of testing various aspects of the quantized-field-quantized-atom interaction [1–14]; while the one-atom-one-mode model of Jaynes and Cummings [15] used to describe the strictly one-atom micromaser, as well as the N -atom-one-mode model [16] for those cases where more than one atom is in the cavity at the same time, are of fundamental interest in the theory of exactly solvable quantum models [11,17–19]. Despite, for example, a recent operator equations of motions study of the dynamics of these micromasers [19], the body of theoretical investigations has been largely based on the characteristic properties of the cavity field averaged over the states of the atoms leaving the cavity. However, because of the practical difficulties associated with measuring the states of this cavity field, these theoretical predictions can not be checked experimentally directly. In the experiments, the measurements are actually made on the states of the atoms leaving the cavity [11,14,20–22]. The properties of the cavity field must then be inferred from the statistics of the states of the outcoming atoms. It is, therefore, essential to know the relationship between the field statistics and this atomic statistics. This relationship, evidently, requires the knowledge of not only the field statistics but also that of the atomic statistics.

The atomic statistics in the micromaser, namely the outcoming atom statistics, refers to the probability distribution functions for observing the atoms in one state or the other after they have left the cavity. These functions can obviously be found by repeatedly monitoring

these states, either for a fixed number N of the atoms pumped into the cavity and subsequently leaving it or for the atoms pumped for a fixed duration t of time and subsequently collected in that time. The two descriptions are evidently equivalent if the time interval between the successive atoms entering the cavity is a fixed number but not if that time interval is a random variable. The dynamics of the cavity field can similarly be described either as a function of the number N of atoms traversing the cavity or as a function of total passage time t . Of particular interest is the asymptotic, i.e., the steady state, behaviors of the system. The meaning of these asymptotic limits must, of course, depend upon the chosen description: the limit corresponds to the limit $N \rightarrow \infty$ if the dynamics is described in terms of the number of atoms and it corresponds to the limit $t \rightarrow \infty$ if the dynamics is described in terms of the collection time. However, it has already been shown [8] that the density matrix of the cavity field in both of these limits is the same.

The atomic statistics of the micromaser, on the other hand, has only been studied in terms of the atoms collected in a fixed interval of time and that too in the ‘coarse-grained’ description of the equations of motion for the cavity field density operator ρ_f [11,23–29]. However, and despite the fact that coarse-graining appears to involve a coarse averaging over the successive entries of the atoms [11,23], it has been known [30] that when the probability distribution of the intervals between successive atoms entering the cavity is exponential, i.e., when the pumping mechanism is Poissonian, coarse-graining which assumes a steady rate R (say) of entry for the atoms, is precisely equivalent to assuming this strictly Poissonian pumping of the atoms with the same mean rate R . The refs. [25–29] for example adopt this coarse-

grained description from the outset and then collect the outcoming atoms in a fixed interval of time. It is therefore of interest to see whether or not these two alternative descriptions of a fixed number N of atoms collected or of a fixed time t for that collection are asymptotically equivalent in terms of the outcoming atom statistics rather than the field statistics for a general pumping statistics which includes Poissonian pumping only as a special case. Moreover, and despite the fundamental interest of this problem to ergodic theory, insofar as these two limits prove to be different (and they do) there is the possibility at the level of actual experiment of gaining additional information by collecting at fixed N on the one hand and at fixed t on the other. We shall see that this additional information can be helpful in determining the actual state of the cavity field in the micromaser. Thus it is this general question, of fixed N or of fixed t , which is the question addressed in this paper.

In this paper we find the probability of the occupation of the two atomic states (to be called $|e\rangle$, excited and $|g\rangle$, ground) for a fixed number N of atoms leaving the cavity and we find the same probability for the group of atoms collected in a fixed time t . We shall assume the pumping mechanism is binomial. Both regular and Poissonian pumping are then special cases of this binomial pumping. We shall evaluate the parameters Q for these two different cases: Q takes the form of Mandel's 'Q-parameter' [31] and is a measure of the deviation of the variance for the population of a given state from the value it would have if the distribution of that population were Poissonian. We shall find that these Q -parameters for each of the two states are generally different in the two asymptotic limits, the limits $N \rightarrow \infty$ and $t \rightarrow \infty$. We investigate the dependence of these differences on the parameter N_{ex} where N_{ex} is the average number of atoms entering the cavity in one decay time of that cavity. The Q -parameters Q_e for the excited state $|e\rangle$ are found to be different for all N_{ex} in these two asymptotic limits. However, the Q -parameters Q_g for the lower state $|g\rangle$ are different in the two asymptotic limits for small N_{ex} but those differences gradually disappear with an increase in N_{ex} . The value of N_{ex} after which the differences between the two asymptotic results become insignificant are found to depend upon the interaction time. At zero temperature it is Q_e for a fixed number N of atoms as $N \rightarrow \infty$ which closely follows Q_f the Q -parameter for the cavity field: but at finite temperatures this close relationship changes significantly. These observations concern only the low lying trapping states: for other equilibrium states of the cavity field Q_e joins substantially in its behavior with the behavior of the other Q 's even at zero temperature.

The paper is organized as follows:- By following the stroboscopic description, we derive in section II expressions for the joint probability of finding sets of successively entering atoms in a particular sequence of detected states. We also derive a number of alternative stroboscopic maps connecting successive states of the cavity

field, and which have taken into account as an ensemble average the different sequences of atomic state detections. From these in the continuous time i.e., Poisson limit of the input statistics we derive master equations for the field density operator for fixed N . From this result we can regain the usual coarse-grained master equation for the field density operator. In the section III we use the joint probability found in section II to find the joint probability of detecting given numbers of atoms in each of the two states on the passage of N active atoms and from it the variances in the number of atoms detected in a given state. We also find the joint probability of detecting given numbers of atoms in the two states for a fixed collection time t of the atoms and from this determine the variances for the atoms collected in the fixed time t . Numerical results comparing the two descriptions are then presented in the section IV. In an Appendix we outline a method for calculating Q_e and Q_g for fixed N and the corresponding \tilde{Q}_e and \tilde{Q}_g for fixed t .

II. JOINT PROBABILITY FOR STATE DETECTION OF SUCCESSIVE ATOMS

In this section we derive an expression for the joint probability for detecting each of a set of successively entering atoms in either one of their two states after they have left the micromaser cavity.

We consider the usual micromaser system in which a high- Q cavity is pumped by Rydberg atoms at a rate R so low that almost always there is at most one atom at a time in the cavity. We assume that the atoms enter the cavity prepared in the state $|e\rangle$ which is coupled resonantly by a cavity mode of frequency ω_0 to a lower energy state $|g\rangle$ which, for the sake of convenience, we refer to as the ground state. The interaction between such an atom and the e.m. field as the atom traverses the cavity is governed by the Jaynes-Cummings Hamiltonian [15]

$$H = \hbar \left[\omega_0 a^\dagger a + \omega_0 S_z + g \left(a^\dagger S_- + S_+ a \right) \right], \quad (2.1)$$

where (a, a^\dagger) are the field annihilation and creation operators which obey the commutation relation $[a, a^\dagger] = 1$ for bosons (they satisfy the Heisenberg-Weyl algebra [11,19]); operators $S_+ = |e\rangle\langle g|$, $S_- = |g\rangle\langle e|$, $S_z = (1/2)[|e\rangle\langle e| - |g\rangle\langle g|]$ are the atomic operators (and satisfy the su(2) Lie algebra for total spin $S = \frac{1}{2}$ [11,19]), and g is the atom-field coupling constant. The cavity field and the atoms interact also with a heat-bath held at a constant temperature. This coupling induces the excited atomic state to decay spontaneously and to the decay of the cavity field. However, the time for the spontaneous decay between two Rydberg levels, which are the levels of interest here, is long enough compared with the convenient choices of the times of flight t_{int} of the atoms through the cavity to enable one to ignore, to a very good approximation, the effects of the atomic coupling to the thermal reservoir (t_{int} is the interaction time

between the atoms and the cavity field and is $\sim 35\mu\text{ s}$ [20]). Moreover the coupling of the cavity field to the heat-bath may also be ignored during this atom-transit time t_{int} because this time is several orders of magnitude smaller than the decay time T_c of the cavity field ($T_c \sim 0.2\text{ s}$ [20]). Together these two acceptable approximations mean that the dynamical evolution is simply unitary under the Hamiltonian H given by (2.1) during the short time t_{int} . Note that the micromaser system has been studied numerically and in depth during this short atomic transit time t_{int} with the coupling of the field to the heat-bath included [10–12] and it has also been studied analytically [11,32–34]. Analytical results for the Jaynes-Cummings Hamiltonian (2.1) coupled to the heat-bath have also been given in ref. [35] in a different context. All of these studies together confirm the fact that the coupling to the heat-bath does not play any significant role if t_{int} is short enough compared with the atomic and field damping times. As noted this is the case, for example, in the experiments of ref. [20]—although [11] reports some small differences (of the order of percent) from Meystre’s formula [1] for the probability of finding n photons in the cavity mode even when $N = 6000$ atoms have passed through the cavity for parameters within this experimental range. The numerical work [11] is essentially exact and the differences of the order of percent are compatible with the errors involved in the second of the two approximations itemized above together with the approximation $t_{i+1} - t_i - t_{int} \approx t_{i+1} - t_i$ made below; however $N = 6000$ atoms may still not be close enough to equilibrium.

Still, whatever the exact situation for the short time t_{int} , the coupling of the field with the heat-bath must certainly never be ignored during the time intervals between the arrivals of two consecutive atoms into the cavity—for these time intervals are usually significant as compared with the damping time of the field. If the heat-bath has an average of \bar{n} thermal photons at the cavity frequency ω_0 and if $2\kappa \equiv T_c^{-1}$ is the rate of loss of photons then the evolution of the density matrix ρ_f of the field due to its interaction with the thermal reservoir is governed by the usual master equation taken in the rotating frame (cf. e.g., [11] and references) which is

$$\begin{aligned} \frac{d\rho_f}{dt} &= \kappa[(\bar{n} + 1)(2a\rho_f a^\dagger - a^\dagger a\rho_f - \rho_f a^\dagger a) \\ &\quad + \bar{n}(2a^\dagger \rho_f a - a a^\dagger \rho_f - \rho_f a a^\dagger)] \\ &\equiv L\rho_f. \end{aligned} \quad (2.2)$$

Note that L is norm preserving i.e., $\frac{d}{dt} Tr\rho_f = TrL\rho_f = 0$, for the right side is expressible as a sum of commutators the characteristic form for Markovian dynamics [36] (actually the sum in (2.2) is a sum of double commutators). Now, let $\rho_f(t_i)$ be the density matrix of the cavity field at the time t_i of the entry of the i^{th} atom into the cavity. Since, in this paper, the atoms are assumed to enter the cavity in their excited state $|e\rangle$, it follows that the state of the combined system of the atom and the field at

the time t_i is the outer product of $\rho_f(t_i)$ and $|e\rangle\langle e|$. The system then evolves, as discussed above, under the action of the Hamiltonian (2.1) alone for the time t_{int} —the time of flight of the atom through the cavity. It can then be shown that under this unitary evolution during t_{int} the density matrix $\rho(t_i + t_{int})$ of the combined system as the i^{th} atom leaves the cavity is given by

$$\begin{aligned} \rho(t_i + t_{int}) &= [F_e(t_{int})|e\rangle\langle e| + F_g(t_{int})|g\rangle\langle g| \\ &\quad + F_{eg}(t_{int})|e\rangle\langle g| + F_{eg}^\dagger(t_{int})|g\rangle\langle e|] \rho_f(t_i) \end{aligned} \quad (2.3)$$

where

$$\begin{aligned} F_e(t_{int})\rho_f(t_i) &= \cos(gt_{int}\sqrt{a^\dagger a + 1})\rho_f(t_i) \\ &\quad \times \cos(gt_{int}\sqrt{a^\dagger a + 1}), \\ F_g(t_{int})\rho_f(t_i) &= a^\dagger \frac{1}{\sqrt{a^\dagger a + 1}} \sin(gt_{int}\sqrt{a^\dagger a + 1})\rho_f(t_i) \\ &\quad \times \sin(gt_{int}\sqrt{a^\dagger a + 1}) \frac{1}{\sqrt{a^\dagger a + 1}} a, \\ F_{eg}(t_{int})\rho_f(t_i) &= i \cos(gt_{int}\sqrt{a^\dagger a + 1})\rho_f(t_i) \\ &\quad \times \sin(gt_{int}\sqrt{a^\dagger a + 1}) \frac{1}{\sqrt{a^\dagger a + 1}} a. \end{aligned} \quad (2.4)$$

Significant quantities are, e.g. [1,11,23,24,32,35]

$$\beta_m = \sin^2(gt_{int}\sqrt{m}) = 1 - \alpha_m. \quad (2.5)$$

The quantity β_{m+1} is the *a priori* probability that an excited atom after traversing the cavity containing m photons would exit it in its ground state and α_{m+1} is the probability of exiting in its excited state (cf. e.g., [37]). The expression (2.3) shows that the actual probability $P(e; t_i)$ ($P(g; t_i)$) that the i^{th} atom exits the cavity in the excited (ground) state is

$$\begin{aligned} P(e; t_i) &= Tr_f[F_e\rho_f(t_i)], \\ (P(g; t_i) &= Tr_f[F_g\rho_f(t_i)]), \end{aligned} \quad (2.6)$$

where Tr_f denotes the operation of trace over the field.

After leaving the cavity, the atom passes through a detector which determines its state. We assume that the time that the atom takes to arrive at the detector after leaving the cavity is small enough for any losses that the atom may suffer due to spontaneous emission can be ignored. However, the probability of detection of the atom in either state may still not be the same as the probability with which it leaves the cavity in that state. This is because the detector may not be of unit efficiency. Following ref. [21], for example, we assume that the detector has an efficiency η_e (η_g) for detecting an atom in its excited (ground) state. Clearly, the probability $P_d(e; t_i)$ ($P_d(g; t_i)$) that the i^{th} atom is detected in the state $|e\rangle$ ($|g\rangle$) after leaving the cavity is then given by

$$\begin{aligned}
P_d(\nu_i; t_i) &= \eta_{\nu_i} P(\nu_i; t_i) \\
&\equiv \text{Tr}[F_{\nu_i, d} \rho_f(t_i)], \quad \nu_i = e, g
\end{aligned} \tag{2.7}$$

where $P(e; t_i)$ ($P(g; t_i)$) is the probability, given by (2.6), that the atom leaves the cavity in the state $|e\rangle$ ($|g\rangle$) and

$$F_{\nu, d} = \eta_{\nu} F_{\nu}, \quad \nu = e, g. \tag{2.8}$$

Here, we have introduced the subscript d on those probabilities and operators which depend on the detector efficiency and $F_{\nu, d}$, like F_{ν} , depends on t_{int} as in (2.4). Since the detector efficiency is not necessarily unity, there is a finite probability that the atom passes through the detector without its state being detected. It is straightforward to see that the probability $P_d(n; t_i)$ that the atom goes through without any state detection is

$$P_d(n; t_i) = \text{Tr}[F_{n, d} \rho_f(t_i)], \tag{2.9}$$

where

$$F_{n, d} = (1 - \eta_e) F_e + (1 - \eta_g) F_g, \tag{2.10}$$

and depends on t_{int} . We have thus evaluated the probability of detection in a given state by (2.7), or of no state detection by (2.9), for an atom as it comes out of the cavity. These expressions (2.7) and (2.9) show that the probability of detecting an atom in one of its states or that of no detection is obtained by operating on the density matrix (density operator) of the field, taken at the time of the entry of that atom, by the operator $F_{\nu, d}$ (now with $\nu = e, g, n$) followed by the operation of trace over the field. Next we use this procedure to find the probability of a particular outcome of the process of state detection for the next, i.e. the $(i+1)^{th}$, atom.

Now, in order to determine the probability of detection or of no detection of a state of the $(i+1)^{th}$ atom on its exit from the cavity, we need to know the state of field at the time t_{i+1} of its entry into the cavity. Since the i^{th} atom is subjected to detection, the state of the field in the cavity at the time of entry of the $(i+1)^{th}$ atom is conveniently described by the *conditional density operator* $\rho_f(t_{i+1}|\nu_i; t_i)$ [38] which characterizes the field at the time t_{i+1} of entry of the $(i+1)^{th}$ atom into the cavity under the condition that the i^{th} atom, which entered at t_i , is detected at $t_i + t_{int}$ in the excited state $\nu_i = e$, is detected in the ground state $\nu_i = g$, or goes through without any state detection $\nu_i = n$. By following the procedure outlined following equation (2.10) the probability of a particular outcome for the process of detection on the $(i+1)^{th}$ atom is then found to be

$$P_d(\nu_{i+1}; t_{i+1}|\nu_i; t_i) = \text{Tr}_f [F_{\nu_{i+1}, d} \rho_f(t_{i+1}|\nu_i; t_i)]. \tag{2.11}$$

Next we must find the expression for the conditional density operator $\rho_f(t_{i+1}|\nu_i; t_i)$ in terms of the state of the field at the time t_i of the entry of the i^{th} atom. This expression is found by first determining the conditional

density operator $\rho_f(t_i + t_{int}|\nu_i; t_i)$ of the field at the time $t_i + t_{int}$ of the exit of the i^{th} atom.

By comparison with (2.3) it is straightforward to see that the state of the cavity field at the time of exit of the i^{th} atom corresponding to each outcome of its detection is (with dependence on t_{int} included)

$$\rho_f(t_i + t_{int}|\nu_i, t_i) = \frac{F_{\nu_i, d}(t_{int}) \rho_f(t_i)}{P_d(\nu_i; t_i)}, \quad \nu_i = e, g, n. \tag{2.12}$$

After the exit of the i^{th} atom, the density operator (2.12) evolves according to the master equation (2.2) for the time interval $t_{i+1} - t_i - t_{int}$ until the time t_{i+1} when the $(i+1)^{th}$ atom enters. So far in all quantitative micromaser experiments one chooses as far as is possible [39] that $t_{i+1} - t_i \gg t_{int}$. Hence we let $t_{i+1} - t_i - t_{int} \approx t_{i+1} - t_i \equiv \tau_i$. In this way the state of the cavity field at the time t_{i+1} of the entry of the $(i+1)^{th}$ atom is given in terms of the state at the earlier time $t_i + t_{int}$ and in terms of the outcome of the measurement on the atom i by

$$\rho_f(t_{i+1}|\nu_i; t_i) = D(\tau_i) \rho_f(t_i + t_{int}|\nu_i; t_i), \tag{2.13}$$

where

$$D(\tau_i) = \exp(L\tau_i), \tag{2.14}$$

is the formal solution of (2.2). On substituting $\rho_f(t_i + t_{int}|\nu_i; t_i)$ from (2.12) into (2.13) we thus get

$$\rho_f(t_{i+1}|\nu_i; t_i) = \frac{D(\tau_i) F_{\nu_i, d}(t_{int}) \rho_f(t_i)}{P_d(\nu_i; t_i)}, \nu_i = e, g, n; \tag{2.15}$$

for the density operator of the field at the time of the entry of the $(i+1)^{th}$ atom under the condition that the i^{th} atom exits the cavity in the state $|\nu_i\rangle$, $\nu_i = e, g$ or goes undetected ($\nu_i = n$).

The Eq. (2.15) shows that the state of the field at the time of entry of the $(i+1)^{th}$ atom corresponding to a particular outcome of the process of measurement on the i^{th} atom is given by operating on the density matrix at the time of entry of the i^{th} atom by the operator $F_{\nu_i, d}$ ($\nu_i = e, g, n$) followed by operation with the operator D and then normalizing the resulting expression to unit trace.

The desired expression for the conditional probability $P_d(\nu_{i+1}; t_{i+1}|\nu_i; t_i)$ of atomic detection may now be obtained by substituting (2.15) in (2.11). This expression therefore reads

$$P_d(\nu_{i+1}; t_{i+1}|\nu_i; t_i) = \frac{\text{Tr}_f [F_{\nu_{i+1}, d} D(\tau_i) F_{\nu_i, d} \rho_f(t_i)]}{P_d(\nu_i; t_i)}. \tag{2.16}$$

In what follows we require the joint probability $P(\nu_{i+1}; t_{i+1}, \nu_i; t_i)$ that the outcome of the process of detection on the i^{th} atom is ν_i together with the outcome

for the $(i + 1)^{th}$ atom being ν_{i+1} . This probability can be obtained by using the relationship

$$P_d(\nu_{i+1}; t_{i+1}, \nu_i; t_i) = P(\nu_{i+1}; t_{i+1} | \nu_i; t_i) P_d(\nu_i; t_i), \quad (2.17)$$

between the joint and the conditional probabilities. On combining (2.16) and (2.17) we find the desired expression

$$P_d(\nu_{i+1}; t_{i+1}, \nu_i; t_i) = Tr_f [F_{\nu_{i+1}, d} D(\tau_i) F_{\nu_i, d} \rho_f(t_i)], \quad (2.18)$$

for the joint probability of a particular pair of outcomes as a result of measurement on two successive atoms entering the cavity at times t_i and t_{i+1} . We can now repeat the preceding arguments and show that the joint probability $P_d(\nu_N; t_N, \dots, \nu_2; t_2, \nu_1; t_1) \equiv P_d(\{\nu_k; t_k\}_N)$ that the outcome of measurements at their exits on the atoms entering the cavity at times t_1, t_2, \dots, t_N is $\nu_1, \nu_2, \dots, \nu_N$ is given by

$$P_d(\{\nu_k; t_k\}_N) = Tr_f [F_{\nu_N, d} D(\tau_{N-1}) F_{\nu_{N-1}, d} \dots \dots D(\tau_2) F_{\nu_2, d} D(\tau_1) F_{\nu_1, d} \rho_f(t_1)], \quad (2.19)$$

where $\rho_f(t_1)$ is the density operator of the field at the time of entry of first atom into the cavity.

Similarly, by following the procedure outlined after (2.15), the state of the cavity field at the time t_N of the entry of the N^{th} atom is described by the conditional density operator

$$\rho_f(t_N | \{\nu_k; t_k\}_{N-1}) = \frac{[D(\tau_{N-1}) F_{\nu_{N-1}, d} \dots D(\tau_1) F_{\nu_1, d} \rho_f(t_1)]}{P_d(\{\nu_k; t_k\}_{N-1})}. \quad (2.20)$$

Note that the density matrix $\rho_f(t_N)$ characterizing the state of the cavity field without any condition on the state of the exiting atoms must be related to the conditional state by the relation

$$\rho_f(t_N) = \sum_{\{\nu_k=e,g,n\}} \rho_f(t_N | \{\nu_k; t_k\}_{N-1}) P_d(\{\nu_k; t_k\}_{N-1}), \quad (2.21)$$

where the summation denotes the sum over all the possible outcomes. On substituting (2.20) in (2.21) we get

$$\rho_f(t_N) = \sum_{\{\nu_k=e,g,n\}} \left[D(\tau_{N-1}) F_{\nu_{N-1}, d} \dots \dots D(\tau_2) F_{\nu_2, d} D(\tau_1) F_{\nu_1, d} \rho_f(t_1) \right]. \quad (2.22)$$

The summation on each of the ν_k for one label k can now be carried out by noting that for each k

$$\sum_{\nu_k=e,g,n} F_{\nu_k, d} \equiv F_{e,d} + F_{g,d} + F_{n,d} = F_e + F_g, \quad (2.23)$$

where the equality follows from the use of (2.7) and (2.10). Note that this step at (2.23) *neatly eliminates* the detector efficiencies η_e, η_g from (2.22). For a first investigation let us now assume that the atoms arrive with a regular spacing τ_p , i.e., τ_i is τ_p for all i . The Eq. (2.22) can then be seen to be exactly

$$\rho_f(t_N) = [D(\tau_p) F_0]^{N-1} \rho_f(t_1), \quad (2.24)$$

where

$$F_0 = F_e + F_g. \quad (2.25)$$

Note from (2.3) that $F_0 \rho(t_i)$ is the density operator of the field at the time of exit of the i^{th} atom if the state of this outgoing atom is left undetermined. Moreover the Eq. (2.24) shows that, as is required by (2.22), *the ensemble averaged field does not depend in any way upon the efficiencies of the detectors.*

The Eq. (2.24) is evidently equivalent to the stroboscopic equation or ‘map’

$$\rho_f(t_{i+1}) = D(\tau_p) F_0 \rho_f(t_i), \quad (2.26)$$

for the regular input as it was used in e.g. ref. [13]. The route by which (2.26) is arrived at here is, of course, not at all the one that is usually followed to reach this expression. The usual derivation (e.g. [13]) does not make any reference, from the outset, to the processes of atomic state measurement. The derivation given above specifically demonstrates the consistency of that approach with that developed here now taking proper account of the process of atomic measurement.

The derivation of (2.26) given above shows actually that, for regular inputs at least, all effects of the atomic state detection processes described by the efficiencies η_i vanish under the ensemble average. Indeed because of (2.23) these efficiencies vanish through the ensemble average (2.22) for $\rho_f(t_N)$ for *any* statistics of the sequence τ_i of successive atomic inputs. For the cavity field therefore, effects of state detection have vanished naturally from the ensemble averaged theory. Actual effects of the detection process via the atoms on the state of the cavity field were envisaged already in [1] and were investigated via numerical methods in [21]; one of the present authors also investigated such effects numerically [11,40] by however studying only single realizations of the atomic inputs—where substantial effects can be discerned [40]. Within coarse-grained theory (that is, equivalently, for continuous time Poisson inputs—see below) such effects of the atomic detection processes on the state of the cavity field were also investigated in [25]. Also within coarse-grained theory, by introducing a remarkable *non-linear* master equation taking account of the outcomes of the atomic measurements the ref. [26] shows how these measurement process effects are ultimately eliminated via the ensemble averaging within this theory. Our step at (2.23) on the ensemble averaged, and usual linear, density operator for the field, shows that quite generally for discrete

time entries of the atoms it is not possible to detect via the atoms any effect of the measurements on the atoms on the state of the cavity field. This last statement follows from the fact that we show in section III how the variances for the observed atom statistics depend only on the ensemble averaged field density operator $\rho_f(t_N)$. Of course this expression $\rho_f(t_N)$, Eq. (2.22), must itself be ensemble averaged over the individual realizations of the sequence τ_i , of the atomic inputs. In the derivation of (2.24) we took the τ_i to be constants, $\tau_i = \tau_p$ for all i . We also assumed even in (2.22) that the interaction time t_{int} was a constant. However, in actual experimental situations, the time difference τ_i between the arrival of successive atoms will not be the same for all the atoms. And even the time of interaction t_{int} of the atoms may vary because different atoms may travel with different speeds. In fact, in practice, the times τ_i and t_{int} must both be taken to be random variables.

In this paper we shall consider only the variations in the pumping time by following the widely used model [1,3] of pumping time fluctuations. According to this model, atoms leave the source oven at regular intervals T (say) and are then prepared in a given excited state $|e\rangle$ with a certain probability p prior to their entering the cavity in that excited state. Thus atoms entering with regular spacings T have only the probability p of being in $|e\rangle$ and only atoms arriving in $|e\rangle$ are effective in determining the dynamics of the micromaser. Even so one may still describe this dynamics in terms of the number K of all the atoms or equivalently in terms of the discrete time $t_K = KT$ that all these K atoms take to arrive in the cavity. Alternatively the dynamics may be described in terms of the number N of atoms entering the cavity specifically in their active excited states $|e\rangle$.

First we find the expression for the joint probability $P_d(\{\nu_k; t_k\}_N, t_K)$ that N atoms enter the cavity in their excited states $|e\rangle$ in time t_K and that the outcome of the measurement on those atoms after they leave the cavity is $\nu_1, \nu_2, \dots, \nu_N$. To find this probability let us assume that the state of the cavity field at the time $t = 0$ is $\rho_f(0)$. Now, assume that the atoms numbered $k_i, i = 1, 2, \dots, N$ are excited to the respective state $|e\rangle$. The probability for this event is obtained by using the fact that the probability of m failures followed by a success in a binomial process in which the probability of a success is p is given by $p(1-p)^m$. The time interval between the arrival of active atoms numbered $i-1$ and i ($i = 1, 2, \dots, N$) is therefore given by $(k_i - k_{i-1})T$ with $k_0 \equiv 1$. The probability $P_d(\{\nu_k; t_k\}_N, t_K)$ can be obtained from (2.19) (i) by replacing the damping operator $D(\tau_i)$ between the atoms numbered i and $i-1$ by $D((k_i - k_{i-1})T)$, (ii) by noting that the field density operator $\rho_f(t_1)$ at the time of the entry of the first active atom is $D((k_1 - 1)T)\rho_f(0)$ and (iii) by performing the summation over all k_i to account for all possible realizations of $\{k_i\}$. It then follows that

$$P_d(\{\nu_k; t_k\}_N, t_K) = p^N (1-p)^{K-N} \sum_{k_N=N}^K \sum_{k_{N-1}=N-1}^{k_N-1} \dots \dots \sum_{k_1=1}^{k_2-1} Tr_f \left[D((K - k_N + 1)T) F_{\nu_N, d} D((k_N - k_{N-1})T) \dots \times F_{\nu_{N-1}, d} \dots D((k_2 - k_1)T) F_{\nu_1, d} D((k_1 - 1)T) \rho_f(0) \right], \quad (2.27)$$

where, for later manipulative convenience, we have multiplied on the left by $D((K - k_N + 1)T)$ the factor appearing under the trace. This does not change the results because of the fact that L is norm preserving and $Tr(L\rho) = 0$ so that

$$Tr(D\rho) = Tr(\rho), \quad (2.28)$$

for any ρ .

The evaluation of (2.27) is facilitated by defining the (probability) generating function

$$f(N, x) = \sum_{K=N}^{\infty} x^K P_d(\{\nu_k; t_k\}_N, t_K), \quad (2.29)$$

so that

$$P_d(\{\nu_k; t_k\}_N, t_K) = \frac{1}{K!} \frac{d^K}{dx^K} f(N, x)|_{x=0}. \quad (2.30)$$

On using the expression (2.27) for $P_d(\{\nu_k; t_k\}_N, t_K)$ in (2.29) and on carrying out the summations over the $\{k_i\}$ and K we get

$$f(N, x) = (px)^N Tr_f [D_p(x) \exp(LT) F_{\nu_N, d} D_p(x) \exp(LT) \times F_{\nu_{N-1}, d} \dots D_p(x) \exp(LT) F_{\nu_1, d} D_p(x) \rho_f(0)], \quad (2.31)$$

where

$$D_p(x) = \frac{1}{1 - x(1-p) \exp(LT)}. \quad (2.32)$$

Note that the joint probability $P_d(\{\nu_k; t_k\}_N)$ for the outcomes $\{\nu_k\}$ on the passage of N active atoms irrespective of the time t_K , obtained from $P_d(\{\nu_k; t_k\}_N, t_K)$ by performing the summation over K , is given by

$$P_d(\{\nu_k; t_k\}_N) = \sum_{K=N}^{\infty} P_d(\{\nu_k; t_k\}_N, t_K) = f(N, 1), \quad (2.33)$$

where the last equality is by virtue of (2.29). The joint probability $P_d(\{\nu_k; t_k\}, t_K)$ for the outcomes $\{\nu_k\}$ in time t_K irrespective of the number of active atoms is obtained, on the other hand, by performing the summation over N in $P_d(\{\nu_k; t_k\}_N, t_K)$, i.e.,

$$P_d(\{\nu_k; t_k\}, t_K) = \sum_{N=0}^K P_d(\{\nu_k; t_k\}_N, t_K). \quad (2.34)$$

We will use (2.33) and (2.34) in the next section to find the probability that a given number of atoms are detected in a given state after the passage of a fixed number N of active atoms irrespective of time or that for a fixed collection time t_K . Here we demonstrate the consistency of the approach developed so far by deriving the equation of evolution for the cavity field averaged over all possible outcomes of detection.

The cavity field averaged over all possible outcomes of detection at the time of entry of the K^{th} atom when N atoms have entered the cavity in their active excited states $|e\rangle$ follows from (2.22) and the considerations outlined above and can be seen to be given by

$$\begin{aligned} \rho_f(N, t_K) &= p^N (1-p)^{K-N} \sum_{\{\nu_i=e,g,n\}} \sum_{k_n=1}^K \sum_{k_{n-1}=1}^{k_n-1} \dots \\ &\dots \sum_{k_1=1}^{k_2-1} \left[D(T(K+1-k_N)) F_{\nu_N,d} D(T(k_N-k_{N-1})) \right. \\ &\left. \times F_{\nu_{N-1},d} \dots D(T(k_2-k_1)) F_{\nu_1,d} D(T(k_1-1)) \rho_f(0) \right]. \end{aligned} \quad (2.35)$$

On carrying out the summation over ν_i in (2.35) by using (2.23) we get

$$\begin{aligned} \rho_f(N, t_K) &= p^N (1-p)^{K-N} \sum_{k_n=1}^K \sum_{k_{n-1}=1}^{k_n-1} \dots \\ &\dots \sum_{k_1=1}^{k_2-1} \left[D(T(K+1-k_N)) F_0 D(T(k_N-k_{N-1})) \right. \\ &\left. \times F_0 \dots D(T(k_2-k_1)) F_0 D(T(k_1-1)) \rho_f(0) \right], \end{aligned} \quad (2.36)$$

where F_0 is again as defined in (2.25) and the averaging over the ν_i has again eliminated the effects of the atomic detection processes. From (2.36) it is now straightforward to derive the recurrence relation

$$\begin{aligned} \rho_f(N, t_{K+1}) &= \exp(LT) \left[(1-p) \rho_f(N, t_K) \right. \\ &\left. + p F_0 \rho_f(N-1, t_K) \right], \end{aligned} \quad (2.37)$$

which in principle determines the ensemble averaged cavity field $\rho_f(N, t_K)$ at the time t_K under the condition that in that time N atoms have entered the cavity in their active excited states $|e\rangle$. Note once more that this ensemble averaged cavity field, relation (2.37) is independent of the detector efficiencies. It can be seen to reduce to (2.26) for regular inputs by setting $p=1$ and $T=\tau_p$.

The relation (2.37) can now be used to determine the field density matrix at the time t_K or at the time of entry of the N^{th} excited atom. The field density matrix $\tilde{\rho}_f(t_K)$ at the time t_K is given by $\rho_f(N, t_K)$, summed over all N , whereas the field density matrix $\rho_f(N)$ after the passage

of a fixed number N of active atoms is given by $\rho_f(N, t_K)$, summed over all K . Now, on performing the summation over N in (2.37) we arrive exactly at the familiar map

$$\tilde{\rho}_f(t_{K+1}) = \exp(LT) \left[(1-p) + p F_0 \right] \tilde{\rho}_f(t_K), \quad (2.38)$$

already derived in ref. [8]. The derivation of (2.38) in [8] was however quite different from that just given now; in [8] no account whatsoever was taken of the sets of measurement on the atoms; here these sets of measurement are fundamental to the whole analysis even though they play no role in the final result. In the same way the summation over K on (2.37) together with a readjustment of the terms leads to the map

$$\rho_f(N+1) = \frac{p \exp(LT) F_0}{1 - (1-p) \exp(LT)} \rho_f(N). \quad (2.39)$$

The relation (2.39) can also be derived from the map (2.26) by assuming that the pumping time τ_p in it is a random variable corresponding to the binomial process and on performing the average over all of its possible realizations. It is this procedure which was followed in ref. [1] in order to derive the equation for the case of strictly Poisson pumping.

Of particular interest is the steady state solution of the maps (2.38) and (2.39). The steady state of the map (2.38) ((2.39)) is the state reached in the asymptotic limit $t_K \rightarrow \infty$ ($N \rightarrow \infty$) and is such that $\tilde{\rho}_f(t_{K+1}) = \tilde{\rho}_f(t_K)$ ($\rho_f(N+1) = \rho_f(N)$). Hence the steady state ρ_{ss} of (2.38) is the solution of the operator equation

$$\left[1 - \exp(LT) \left((1-p) + p F_0 \right) \right] \rho_{ss} = 0. \quad (2.40)$$

However it is easy to see that the steady state of the map (2.39) also obeys (2.40). Hence the steady state density matrix of the cavity field is the same whether the dynamics is described in terms of time or in terms of the number of active atoms traversing the cavity. The exact solution of (2.40) is known only for the case of Poisson pumping discussed next.

A widely studied and experimentally important case of random pumping is Poisson pumping. This corresponds to the limit $p \rightarrow 0$, $T \rightarrow 0$ of binomial pumping such that $p/T \rightarrow R$ where the constant R is the average rate of pumping of the active atoms. In this limit, the atoms enter the cavity continuously. In other words, in the Poisson limit, the discrete time t_K becomes a continuous variable t . Hence one can write $\rho_f(N, t_{K+1}) - \rho_f(N, t_K) = T(d/dt)\rho_f(N, t)$. The recurrence relation (2.37) then reduces to the equation

$$\frac{d}{dt} \rho_f(N, t) = \left[L \rho_f(N, t) + R(F_0 - 1) \rho_f(N-1, t) \right], \quad (2.41)$$

coupling $\rho_f(N, t)$ and $\rho_f(N-1, t)$ and which on iteration determines the evolution of the field at time t under the

condition that N active atoms enter the cavity in that time. The equation for the field density matrix $\tilde{\rho}_f(t)$ at time t irrespective of the number of active atoms can be derived from (2.41) by performing the summation over N . This leads to the exact master equation

$$\frac{d}{dt}\tilde{\rho}_f(t) = \left[L + R(F_0 - 1) \right] \tilde{\rho}_f(t). \quad (2.42)$$

This master equation is the same as the one that is obtained in the coarse-grained approximation without making any reference to the pumping statistics (see for example [26] or [11], [23]—where coarse-grained averages are actually taken). The Eq. (2.42) can also be derived by taking the Poisson limit of (2.38). Finally, the density matrix of the field after the passage of a fixed number N of active atoms, taken irrespective of the time for the case of Poissonian pumping, is found from (2.39) to be given by

$$\rho_f(N+1) = \frac{1}{1-L/R} F_0 \rho_f(N). \quad (2.43)$$

This equation is the same as the one derived in ref. [1] for the Poisson pumping process achieved by starting from (2.26) and assuming the pumping times τ_p to be random variables corresponding to a Poisson process and then performing the average over all realizations of this pumping time.

Now cf. Eq. (2.27) and observe that we have there the exact stroboscopic expression for the probability that N atoms in their active excited state are pumped into the cavity in a given time t_K and that the process of state detection after these atoms exit the cavity gives a particular sequence of outcomes. We can use this expression to study various aspects of the *atomic* statistics including the correlations between the atoms exiting the cavity at different times. We shall study these correlations in a later paper. Here we restrict attention to the study of the probability of detecting a given number of atoms in a given state.

III. DISTRIBUTION FUNCTION FOR ATOMIC STATE POPULATIONS

In the last section we determined at Eq. (2.27) the joint probability $P_d(\{\nu_k; t_k\}_N, t_K)$ for the outcomes $\{\nu_k = e, g, n\}$ as a result of measurement on N excited atoms passing through the cavity in time t_K . Here we use that joint probability to determine the number distribution $w(N_e, N_g, N)$ which is the probability of detecting N_e atoms in the excited state and N_g atoms in the ground state on the passage of N active atoms and also the number distribution $\tilde{w}(N_e, N_g, t_K)$ for a fixed time interval t_K of observation. We use these expressions to find the variances in the number of atoms exiting the cavity in one state or the other.

Recall that the probability $P_d(\{\nu_k; t_k\}_N)$ is the probability that the outcome of state measurement on N atoms passing through the cavity in an arbitrary time is the set $\{\nu_k\}$ ($\nu_k = e, g, n$). This probability is given by (2.33). Now, the probability $w(N_e, N_g, N)$ that N_e atoms are detected in the state $|e\rangle$ and N_g in the state $|g\rangle$ on the passage of N excited atoms is clearly the sum of all those joint probabilities $P_d(\{\nu_k; t_k\}_N)$ ($\nu_k = e, g, n$) in which N_e of the ν 's correspond to the excited state and N_g of the ν 's correspond to the ground state. We know from (2.33) that $P_d(\{\nu_k; t_k\}_N) = f(N, 1)$ where $f(N, x)$ is given by (2.31). It is then straightforward to see that $w(N_e, N_g, N)$ is the coefficient of $y^{N_e} z^{N_g}$ in the expansion of $\text{Tr} \left\{ \left[D_p(1) p \exp(LT) (F_{n,d} + yF_{e,d} + zF_{g,d}) \right]^N D_p(1) \rho_f(0) \right\}$ where $D_p(x)$ is given by (2.32). In other words

$$w(N_e, N_g, N) = \frac{1}{N_e! N_g!} \frac{d^{N_e+N_g}}{dy^{N_e} dz^{N_g}} \text{Tr} \left\{ \left[\Lambda_p \times (F_{n,d} + yF_{e,d} + zF_{g,d}) \right]^N \rho_f(t_1) \right\} \Big|_{y=0}^{z=0}, \quad (3.1)$$

where $\rho_f(t_1) = D_p(1) \rho_f(0)$ is the density operator of the field at the time of entry of the first excited atom,

$$\Lambda_p \equiv D_p(1) p \exp(Lp/R), \quad (3.2)$$

and we have substituted $T = p/R$ where R is the average rate at which the atoms are excited. On substituting for $F_{n,d}$ from (2.10) and on changing the variables y and z to $1-y$ and $1-z$ respectively, one finds (3.1) becomes

$$w(N_e, N_g, N) = \frac{(-)^{(N_e+N_g)}}{N_e! N_g!} \frac{d^{N_e+N_g}}{dy^{N_e} dz^{N_g}} \text{Tr} \left\{ \left[\Lambda_p \times (F_0 - y\eta_e F_e - z\eta_g F_g) \right]^N \rho_f(t_1) \right\} \Big|_{y=1}^{z=1}. \quad (3.3)$$

The distribution for the number of atoms detected in the ground state alone, obtained by summing (3.3) over N_e , thus reads

$$w_g(N_g, N) = \frac{(-)^{N_g}}{N_g!} \frac{d^{N_g}}{dz^{N_g}} \text{Tr} \left\{ \left[\Lambda_p (F_0 - z\eta_g F_g) \right]^N \times \rho_f(t_1) \right\} \Big|_{z=1}, \quad (3.4)$$

together with a similar expression for $w_e(N_e, N)$ in which the quantities with suffix g are replaced by the corresponding ones with suffix e . Note that N_e and N_g are not independent variables, so their distributions are related. For the case of unit detection efficiency for each of the two states, $N = N_e + N_g$ which implies $w_e(N_e, N) = w_g(N - N_e, N)$. On using the easily verifiable relation

$$\frac{1}{k!} \frac{d^k}{dx^k} (A + xB) \Big|_{x=0} = \frac{1}{(N-k)!} \frac{d^{N-k}}{dx^{N-k}} (xA + B) \Big|_{x=0}, \quad (3.5)$$

it can then be verified that $w_g(N_g, N)$ given by (3.4) and the corresponding expression for $w_e(N_e, N)$ indeed satisfy the relation $w_e(N_e, N) = w_g(N - N_e, N)$.

Next we evaluate the atomic population distributions for the case when the observation is made for a fixed time t_K rather than for a fixed number of atoms. The joint probability $P_d(\{\nu_k; t_k\}, t_K)$ for the outcomes of detection in that case is determined by working from (2.34) rather than (2.33). The probability $\tilde{w}(N_e, N_g, t_K)$ that N_e atoms are detected in the state $|e\rangle$ and N_g in the state $|g\rangle$ in time t_K is clearly the sum over all those joint probabilities $P_d(\{\nu_k; t_k\}, K)$ ($\nu_k = e, g, n$) in which N_e of the ν 's correspond to the excited state and N_g of the ν 's correspond to the ground state. With $P_d(\{\nu_k; t_k\}, t_K)$ given by (2.34) taken with (2.30) and (2.31) it follows that

$$\begin{aligned} \tilde{w}(N_e, N_g, t_K) &= \frac{1}{N_e! N_g! K!} \frac{d^{N_e + N_g + K}}{dy^{N_e} dz^{N_g} dx^K} \sum_N (px)^N \\ &\times Tr \left\{ \left[D_p \exp(Lp/R) \left(F_0 - (1-y)\eta_e F_e - (1-z)\eta_g F_g \right) \right]^N \right. \\ &\left. \times D_p \rho_f(0) \right\} \Big|_{x=y=z=0}. \end{aligned} \quad (3.6)$$

Now, on performing the summation over N and on rearranging the terms, one finds that the Eq. (3.6) yields

$$\begin{aligned} \tilde{w}(N_e, N_g, t_K) &= \frac{1}{N_e! N_g! K!} \frac{d^{N_e + N_g + K}}{dy^{N_e} dz^{N_g} dx^K} \\ &\times Tr \left\{ \left[1 - x \exp(Lp/R) \left(1 - p + p(F_0 - (1-y)\eta_e F_e \right. \right. \right. \\ &\left. \left. \left. - (1-z)\eta_g F_g \right) \right)^{-1} \rho_f(0) \right] \right\} \Big|_{x=y=z=0}. \end{aligned} \quad (3.7)$$

The differentiation with respect to x can now be performed trivially to get

$$\begin{aligned} \tilde{w}(N_e, N_g, t) &= \frac{(-)^{N_g + N_e}}{N_e! N_g!} \frac{d^{N_e + N_g}}{dy^{N_e} dz^{N_g}} Tr \left\{ \left[\tilde{\Lambda}_p \right. \right. \\ &\left. \left. \left(\tilde{F}_0 - p(y\eta_e F_e + z\eta_g F_g) \right) \right]^{Rt/p} \rho_f(0) \right\} \Big|_{y=1}^{z=1}, \end{aligned} \quad (3.8)$$

where

$$\tilde{\Lambda}_p \equiv \exp(Lp/R), \quad \tilde{F}_0 \equiv 1 - p + pF_0. \quad (3.9)$$

We have replaced t_K by t and substituted $K = t_K/T = Rt/p$. The probability of detecting N_g atoms in the ground state irrespective of the number of atoms in the upper state in time t , found by performing the summation over N_e in (3.8), then reads

$$\begin{aligned} \tilde{w}_g(N_g, t) &= \frac{(-)^{N_g}}{N_g!} \frac{d^{N_g}}{dz^{N_g}} Tr \left[\tilde{\Lambda} \left(\tilde{F}_0 - zp\eta_g F_g \right)^{Rt/p} \right. \\ &\left. \times \rho_f(0) \right] \Big|_{z=1}, \end{aligned} \quad (3.10)$$

in which $\tilde{\Lambda} \equiv \tilde{\Lambda}_p$ and there is a similar expression for $\tilde{w}_e(N_e, t)$ obtained by replacing the quantities with the suffix g by the corresponding ones with the suffix e .

In the continuous time Poisson limit $p \rightarrow 0$ we recover from (3.8) for fixed t the expression

$$\begin{aligned} \tilde{w}(N_e, N_g, t) &= \frac{(-)^{N_g + N_e}}{N_e! N_g!} \frac{d^{N_e + N_g}}{dy^{N_e} dz^{N_g}} Tr \left\{ \exp \left[\left(L + R(F_0 - 1) \right. \right. \right. \\ &\left. \left. \left. - yR\eta_e F_e - zR\eta_g F_g \right) t \right] \rho_f(0) \right\} \Big|_{y=1}^{z=1}, \end{aligned} \quad (3.11)$$

derived in ref. [26] by their very different methods. The expressions for $\tilde{w}_g(N_g, t)$ and $\tilde{w}_e(N_e, t)$ given in [26] are similarly recovered in the Poisson limit of (3.10) and from the Poisson limit of the corresponding expression for $\tilde{w}_e(N_e, t)$.

Next we use the number distributions to find the variances in the numbers of atoms detected in one state or the other. It is straightforward to see from the expressions for $w_g(N_g, N)$ and $\tilde{w}_e(N_e, t)$ that at fixed N for the ground states $|g\rangle$

$$\langle N_g \rangle_N = -\frac{d}{dz} Tr \left\{ \left[\Lambda \left(F_0 - z\eta_g F_g \right) \right]^N \rho_f(t_1) \right\} \Big|_{z=1}, \quad (3.12)$$

and that

$$\langle N_g(N_g - 1) \rangle_N = \frac{d^2}{dz^2} Tr \left\{ \left[\Lambda \left(F_0 - z\eta_g F_g \right) \right]^N \rho_f(t_1) \right\} \Big|_{z=1}, \quad (3.13)$$

in which $\Lambda \equiv \Lambda_p$ while there are similar expressions for the excited states $|e\rangle$ obtained by replacing the quantities with the index g by the corresponding ones with the index e . The corresponding expressions for a fixed observation time t are given by

$$\langle N_g \rangle_t = -\frac{d}{dz} Tr \left\{ \left[\tilde{\Lambda} \left(\tilde{F}_0 - zp\eta_g F_g \right) \right]^{Rt/p} \rho_f(0) \right\} \Big|_{z=1}, \quad (3.14)$$

and

$$\langle N_g(N_g - 1) \rangle_t = \frac{d^2}{dz^2} Tr \left\{ \left[\tilde{\Lambda} \left(\tilde{F}_0 - zp\eta_g F_g \right) \right]^{Rt/p} \rho_f(0) \right\} \Big|_{z=1}. \quad (3.15)$$

with similar expressions for e rather than g . We use (3.12)–(3.15) to evaluate the parameters Q_g defined in Mandel's [31] Q -parameter form by

$$Q_g = \frac{\langle N_g(N_g - 1) \rangle}{\langle N_g \rangle^2} - \langle N_g \rangle. \quad (3.16)$$

Definition (3.16) has a similar form for Q_e with e replacing g . These quantities (3.16) are measures of the deviation of the observed distribution from a Poisson distribution. The values $Q_g = 0$ means that the corresponding statistical distribution is Poissonian; $Q_g < 0$ and $Q_g > 0$ imply sub- and super-Poissonian distributions respectively. An approximate relationship between Q_g and Q_f the corresponding Q -function for the cavity field both evaluated for fixed t is derived in ref. [21]. However this relation has since been found to be of limited validity [25,26]. The numerical calculations described in the next section for both fixed t and fixed N lead us to a similar conclusion.

Now, the operations of differentiation in (3.12)–(3.15) can be performed by using the easily verifiable results that

$$\frac{d}{dx}(A + xB)^n = \sum_{k=0}^{n-1} (A + xB)^k B(A + xB)^{n-k-1}, \quad (3.17)$$

and

$$\begin{aligned} \frac{d^2}{dx^2}(A + xB)^n &= \sum_{k,l} [(A + xB)^l B(A + xB)^{k-l-1} \\ &\times B(A + xB)^{n-k-1} + (A + xB)^k B(A + xB)^l \\ &\times B(A + xB)^{n-k-l-2}]. \end{aligned} \quad (3.18)$$

In this paper we shall evaluate (3.12)–(3.15) by assuming, in accordance with ref. [26], that the system is initially in the steady state, i.e., $\rho_f(t_1) = \rho_f(0) = \rho_{ss}$ where ρ_{ss} is the solution of (2.40). We make use of the fact that D_p and F_0 are both trace conserving, i.e.,

$$Tr_f[D_p \rho] = Tr_f[\rho], \quad Tr_f[F_0 \rho] = Tr_f[\rho], \quad (3.19)$$

for an arbitrary ρ . On evaluating (3.12) and (3.13) and substituting the resulting expressions in (3.16) one finds

$$\langle N_g \rangle_N = \eta_g N Tr_f[F_g \rho_{ss}], \quad (3.20)$$

and

$$\begin{aligned} Q_g &= \frac{2\eta_g}{Tr_f[F_g \rho_{ss}]} Tr_f \left[F_g \left(1 - \frac{1 - (\Lambda_p F_0)^N}{N(1 - \Lambda_p F_0)} \right) \right. \\ &\times \left. \left(\frac{1}{1 - \Lambda_p F_0} \right) \Lambda_p F_g \rho_{ss} \right] - \eta_g N Tr_f[F_g \rho_{ss}], \end{aligned} \quad (3.21)$$

which is the desired expression for Q_g with particular reference to the detection of atoms in the ground state $|g\rangle$ for a fixed number N of excited atoms entering the cavity in an arbitrary time. Similarly, in the case when the observation is made for a fixed time t the expressions (3.14) and (3.15) yield

$$\langle N_g \rangle_t = \eta_g R t Tr_f[F_g \rho_{ss}] \quad (3.22)$$

and

$$\begin{aligned} \tilde{Q}_g &= \frac{2\eta_g p^2}{Tr_f[F_g \rho_{ss}]} Tr_f \left[F_g \left(\frac{1}{p} - \frac{1 - (\tilde{\Lambda}_p \tilde{F}_0)^{Rt/p}}{Rt(1 - \tilde{\Lambda}_p \tilde{F}_0)} \right) \right. \\ &\times \left. \left(\frac{1}{1 - \tilde{\Lambda}_p \tilde{F}_0} \right) \tilde{\Lambda}_p F_g \rho_{ss} \right] - \eta_g R t Tr_f[F_g \rho_{ss}], \end{aligned} \quad (3.23)$$

where the tilde on the Q now means fixed collection time t . In the Poisson limit $p \rightarrow 0$, (3.22) and (3.23) reduce to the corresponding expressions derived for fixed t in ref. [26]. The expressions for Q_e and \tilde{Q}_e are obtained by replacing the quantities with suffix g by the corresponding ones with suffix e in (3.21) and (3.23) respectively. Note that all of these Q -functions are directly proportional to the corresponding detector efficiencies for any choice of p , thus solving the problem raised, for example, in [21] and, for $p \rightarrow 0$ and fixed t in agreement with [26].

We outline in the Appendix a method of actually evaluating these Q -functions (3.21) and (3.23) for both of e and g .

We have already shown in the last section (at (2.40)) that the state of the *field* observed after the passage of a large number N of active atoms is the same as the one observed after waiting for a long time. We now find the atomic Q -functions for a group of a fixed number $N \rightarrow \infty$ of atoms using (3.21) and for a group of atoms passing through the cavity in a fixed time $t \rightarrow \infty$ by evaluating (3.23) in the limit $t \rightarrow \infty$. The results of the numerical computations are presented in the next section.

Here we compare the predictions of the two approaches in the case of an analytically solvable example. This is the example of the micromaser operating without any thermal photons ($\bar{n} = 0$ in (2.2)) and having an interaction time such that $gt_{int} = \pi/\sqrt{2}$. In this case the Fock state $|1\rangle$ is a trapping state [4]. Hence, if the cavity field is initially in the state of vacuum then the state of the micromaser is described by two-dimensional matrices and this makes the problem analytically tractable. We find the Q -functions for the upper and the lower states in the limit $t \rightarrow \infty$ to be given by the formulae

$$\begin{aligned} \tilde{Q}_e &= \frac{-\eta_e}{1 - d + p\beta_1 d} \left(\frac{2p^2 \beta_1^2 (1 - d)(\alpha_1 + p\beta_1 d - d)d}{(1 - d + p\beta_1 d)[\alpha_1(1 - d) + p\beta_0 d]} \right. \\ &\left. + p[\alpha_1(1 - d) + p\beta_1 d] \right), \end{aligned} \quad (3.24)$$

and

$$\begin{aligned} \tilde{Q}_g &= \frac{-\eta_g}{1 - d + p\beta_1 d} \left(\frac{2p\beta_1(1 - p\beta_1)(1 - d)d}{1 - d + p\beta_1 d} \right. \\ &\left. + p\beta_1(1 - d) \right), \end{aligned} \quad (3.25)$$

where

$$\begin{aligned} d &= \exp\left(-\frac{p}{N_{ex}}\right), \\ \beta_1 &= 1 - \alpha_1 = \sin^2\left(\frac{\pi}{\sqrt{2}}\right), \\ N_{ex} &= \frac{R}{2\kappa}. \end{aligned} \quad (3.26)$$

The parameter N_{ex} is the usual so-called pumping parameter mentioned in the abstract which gives the average number of atoms pumped into the cavity in one cavity damping time. Note from (3.25) that \tilde{Q}_g is always negative, i.e., sub-Poissonian whereas \tilde{Q}_e is definitely sub-Poissonian if $\alpha_1 + p\beta_1 d - d > 0$. For the particular case of Poisson pumping statistics the limit $p \rightarrow 0$ in (3.24) and (3.25) yields

$$\tilde{Q}_e = \frac{2\eta_e\beta_1^3 N_{ex}^2}{(N_{ex}\beta_1 + \alpha_1)(N_{ex}\beta_1 + 1)^2}, \quad (3.27)$$

and

$$\tilde{Q}_g = \frac{-2\eta_e\beta_1 N_{ex}}{(N_{ex}\beta_1 + 1)^2}. \quad (3.28)$$

These expressions (3.27) and (3.28) for fixed $t \rightarrow \infty$ and $p \rightarrow 0$ are exactly the same as the corresponding ones derived in ref. [26]. Thus, in the case of Poisson pumping, the atoms exiting the cavity in the upper state follow a super-Poisson distribution whereas those emerging in the lower state have a strictly sub-Poissonian distribution.

In a similar way the Q -functions in the limit $N \rightarrow \infty$ are found to be given by

$$Q_e = \frac{-\eta_e}{1-d+p\beta_1 d} \left(\frac{2p\beta_1^2\alpha_1(1-d)^2 d}{(1-d+p\beta_1 d)[\alpha_1(1-d)+p\beta_1 d]} + \alpha_1(1-d) + p\beta_1 d \right). \quad (3.29)$$

and

$$Q_g = \frac{-\eta_g}{1-d+p\beta_1 d} \left(\frac{2p\beta_1\alpha_1(1-d)d}{1-d+p\beta_1 d} + \beta_1(1-d) \right). \quad (3.30)$$

Note that in this case, i.e., in the case of observations made on groups of a fixed large number N of atoms as $N \rightarrow \infty$, both Q_e as well as Q_g are sub-Poissonian. In the Poisson limit $p \rightarrow 0$, (3.29) and (3.30) reduce to

$$Q_e = \frac{-\eta_e}{\beta_1 N_{ex} + 1} \left(\frac{2\beta_1^2\alpha_1 N_{ex}}{(\beta_1 N_{ex} + 1)(\beta_1 N_{ex} + \alpha_1)} + \beta_1 N_{ex} + \alpha_1 \right), \quad (3.31)$$

and

$$Q_g = \frac{-\eta_g}{\beta_1 N_{ex} + 1} \left(\frac{2\beta_1\alpha_1 N_{ex}}{(\beta_1 N_{ex} + 1)} + \beta_1 \right). \quad (3.32)$$

The differences between the atomic statistics in the long time and the large number of atoms limits are clearly reflected in these various analytical results.

It is instructive to consider the behavior of the Q -functions derived above for the special cases of the micro-maser with low and high rates of pumping respectively. For the low rate of pumping R (or equivalently high rate κ of field damping), $N_{ex} \rightarrow 0$. In this limit $\langle N_g \rangle \rightarrow N\eta_g\beta_1$,

$\langle N_e \rangle \rightarrow N\eta_e(1-\beta_1)$, $Q_g \rightarrow -\eta_g\beta_1$, $Q_e \rightarrow -\eta_e(1-\beta_1)$. These values of $\langle N_g \rangle$ ($\langle N_e \rangle$) and Q_g (Q_e) correspond to a binomial process in which the probability of success is β_g ($[1-\beta_g]$) (see (4.1) below). Hence it follows that the statistics of the atomic populations exiting the cavity is binomial irrespective of the pumping statistics if the observations are made on groups of a fixed number, $N \rightarrow \infty$, of atoms. If, on the other hand, the observations are made for fixed time, $t \rightarrow \infty$ then the desired averages are obtained from the corresponding ones for groups of fixed number N of atoms by averaging over N with the probability that N atoms exit the cavity in time t . In this case, for the present example, $\langle N_g \rangle$ ($\langle N_e \rangle$) and Q_g (Q_e) are expected to be $Rt\eta_g\beta_1$ ($Rt\eta_e[1-\beta_1]$), and $-p\eta_g\beta_1$ ($-p\eta_e[1-\beta_1]$) [see (4.2)]. It is easy to see that (3.24) and (3.25) indeed yield those results in the limit $N_{ex} \rightarrow 0$, so that $d \rightarrow 0$.

Next, for $N_{ex} \rightarrow \infty$, that is in the limit of a high rate of pumping or equivalently of a low rate of field losses (namely for an ideal cavity), one has $Q_e \rightarrow -1$, $\tilde{Q}_e \rightarrow -p$, $Q_g \rightarrow \tilde{Q}_g \rightarrow 0$. These are evidently precisely the values of the Q -parameters for the atoms entering the cavity. This behavior of the Q -parameters can be readily understood by noting that in this limit, the steady state of the field is the trapping state $|1\rangle$: the atoms therefore exit the cavity in their upper states $|e\rangle$ which are the states in which they enter the cavity. Hence, in the limit $N_{ex} \rightarrow \infty$, the statistics of the atoms exiting the cavity is exactly the same as the pumping statistics.

In the next section we investigate in detail the differences between the atomic statistics in the long time and in the large N limit by numerical evaluation of not only the analytical expressions for the Q -functions for the special case of $gt_{int} = \pi/\sqrt{2}$ at zero temperature discussed above, but also for several other gt_{int} 's defining both trapping states and non-trapping states [43] at both zero and finite temperatures.

IV. NUMERICAL RESULTS AND DISCUSSION

In this section we present numerical evaluations of the atomic Q functions in the asymptotic limits $N \rightarrow \infty$ and $t \rightarrow \infty$. Since the efficiency factors appear only as a multiplicative factor we give the results only for unit efficiencies $\eta_e = \eta_g = 1$.

The parameter Q_e (Q_g) is obviously the same as \tilde{Q}_e (\tilde{Q}_g) for the case of regular pumping $p = 1$. We, therefore, examine these parameters first for $p = 0$ (Poisson pumping) for this corresponds to a maximum departure from the regular input. We display first in Fig. 1 the plots of Q_e , Q_g and \tilde{Q}_e , \tilde{Q}_g together with Q_f as functions of the pumping parameter $N_{ex} = R/2\kappa$ in the case of a Poisson input and for which $gt_{int} = \pi/\sqrt{2}$ while the system is at zero temperature, $\bar{n} = 0$. The exact analytical expressions for these Q -parameters were given towards the end of the last section. It is clear from the figure

that Q_e and \tilde{Q}_e differ in the entire range of N_{ex} whereas Q_g and \tilde{Q}_g differ significantly for small N_{ex} but approach each other as N_{ex} is increased. Notice how it is only Q_e which closely follows Q_f . This is because Q_g , \tilde{Q}_e and \tilde{Q}_g all tend to zero with $N_{ex} \rightarrow \infty$ while $Q_e \rightarrow -1$. Notice that as $N_{ex} \rightarrow \infty$ either cavity $Q \rightarrow \infty$ ($2\kappa \rightarrow 0$) or the mean entry rate $R \rightarrow \infty$ (or both). If $R \rightarrow \infty$ the probability of there being more than one atom in the cavity becomes large and the TC-model Hamiltonian [16] must replace the JC-Hamiltonian Eq. (2.1). For $N_{ex} \rightarrow \infty$ we must therefore assume the cavity Q becomes large so as to maintain any relevance to the actual experiments done so far.

We next examine the effect of finite temperatures on the differences in the two kinds of Q -functions by plotting in Fig. 2 the same data as in Fig. 1 but for $\bar{n} = 0.1$. The differences between the two kinds of Q -functions seem to decrease with an increase in \bar{n} . The other point to notice is that Q_e and Q_f were both sub-Poissonian for all N_{ex} and were monotonically decreasing to -1 at zero temperature as in the Fig. 1. These behaviors for both Q_e and Q_f and indeed the behaviors of Q_g , \tilde{Q}_e and \tilde{Q}_g evidently change dramatically with the increase in temperature 0.2 K ($\bar{n} = 0.10$). We return to this in the Figs. 10–13 where these effects of temperature are displayed.

In Fig. 3 we investigate the effects of the departure from the continuous time Poisson statistics on the differences between the two limits by plotting the Q -functions as functions of N_{ex} for the discrete time binomial distribution with $p = 0.5$ for $gt_{int} = \pi/\sqrt{2}$ and $\bar{n} = 0$. Not too much difference from the plots of Fig. 1 can be seen from this significant change of p , except for the observation that \tilde{Q}_e shows sub-Poissonian behavior for the entire range of N_{ex} , whereas for $p = 0$, it was totally super-Poissonian.

Next we plot in Fig. 4 the Q -functions for another value of gt_{int} namely, $gt_{int} = 1.54$ as a function of N_{ex} for $\bar{n} = 0.145$ (temperature = 0.5 K) and for the case of Poissonian pumping. This is the set of parameters used in the experiments of ref. [20]. Once again we find that the two kinds of Q -functions differ considerably and differ considerably from Q_f for small N_{ex} . It is interesting to compare the plot of \tilde{Q}_g with the experimental plot, Fig. 3 of ref. [20]. One can check that the theoretical plot for \tilde{Q}_g given in Fig. 4 here exhibits the minima and the maxima at the same positions as the plot of the experimental points. However, whereas the second minima of the experimental points exhibits sub-Poisson behavior, that of the theoretical plot is super-Poissonian and to this extent the sub-Poissonian field with $Q_f = -0.3$ observed at $N_{ex} = 35$ in \tilde{Q}_g in [20] may need further scrutiny. Note that the numerical values in the two plots, even after correcting for the efficiency factor, do not match at all. The reason for the discrepancy between the two apparently may stem from the fact that there are stray fields present in the experiments (cf. [42]) which have not been taken into account in the theoretical plot of Fig. 4.

In Fig. 5 we plot the same data as in Fig. 4 except that $\bar{n} = 0$ (zero temperature). In view of the Figs. 1 and 2 where $\bar{n} = 0$ and $\bar{n} > 0$ the most striking feature of Fig. 5 ($\bar{n} = 0$) in relation to Fig. 4 ($\bar{n} > 0$) is that qualitatively there is little change, although Q_e for $N_{ex} \sim 44$ is sub-Poissonian and approaching Q_f from Fig. 4 which is also sub-Poissonian for however $N_{ex} \approx 35$. Note that $gt_{int} = 1.54$ is not a low-lying (in terms of photon number n) trapping state.

Notice how the increase in temperature from zero to 0.15 K between the Figs. 5 and 4 pushes all of the Q 's substantially to the left (lower N_{ex}) so that each of the minima of Q_e , \tilde{Q}_e , Q_g , \tilde{Q}_g , of which only Q_e is sub-Poissonian, arise at $N_{ex} \sim 44$ in Fig. 5 while these are pushed to $N_{ex} \sim 35$ in Fig. 4 with now Q_e just super-Poissonian. Apparently the big maximum for the atomic Q 's for $N_{ex} \geq 42$ in Fig. 4 is pushing these minima strongly to the left as described. Notice now that this effect of temperature for $gt_{int} = 1.54$ is *qualitatively* different from the effect of temperature between Fig. 1 and Fig. 2. This is apparently due to the fact that in Figs. 1 and 2, $gt_{int} = \pi/\sqrt{2}$ which is the one-photon trapping state condition: the $gt_{int} = 1.54$ radians does not define any trapping state with a small number of photons. Thus, with $\pi = 3.14159$ for example, one finds that the lowest trapping state has the photon number $n \sim 4 \times 10^{10}$! At zero temperature and $T_c = \infty$ (ideal cavity) the trapping states are the only equilibrium states [13,19]; but although $gt_{int} = 1.54$ at zero temperature in Fig. 5, $T_c < \infty$ and equilibrium is expected to lie below the *lowest* trapping state (in terms of photon number) as was demonstrated in [13]. For lowest trapping states with small photon number switching on the temperature induces a rather remarkable ‘escape’ to the larger photon numbers which leads to the rather dramatic rises in variances evident in the sequence of thresholds for these variances shown in the contrasts between the Figs. 5 and shown below for which figures all are taken at low lying trapping states. A conclusion remains that there is no simple relation between Q_f and any of Q_g , Q_e , \tilde{Q}_g and \tilde{Q}_e at finite temperature while it is only Q_e which follows Q_f relatively closely at zero temperature.

We next examine, in Figs. 6 and 7, the differences in the two kinds of asymptotic limits as a function of gt_{int} for $N_{ex} = 1$ (Fig. 6) and $N_{ex} = 5$ (Fig. 7) for $\bar{n} = 0.1$ and for the case of Poisson pumping. These figures confirm that these differences depend on N_{ex} for any gt_{int} . Thus the curves for Q_e , Q_g differ from the corresponding \tilde{Q}_e , \tilde{Q}_g curves for all gt_{int} for $N_{ex} = 1$ (Fig. 6), while their differences decrease as the values of N_{ex} is increased to 5 (Fig. 7). The Fig. 8 shows these differences for the experimentally realized value of $N_{ex} = 30$. In the Fig. 9 we repeat the data of Fig. 7 at $\bar{n} = 0$ (zero temperature). Low-lying trapping states arise at $gt_{int} = \pi/\sqrt{2}$, $\pi/\sqrt{3}$, $\pi/2$, $\pi/\sqrt{5}$, $\pi/\sqrt{6}$ for example for $r = 1$ in the trapping state condition $gt_{int}\sqrt{\bar{n} + 1} = r\pi$. For $r = 1, 2, 3$ etc. they arise for $gt_{int} = \pi/2$, $\pi/4$,

$\pi/6$ and so on, for example. Still Fig. 7 shows little qualitative change from Fig. 9 ($\bar{n} = 0$).

For the Fig. 10 we note that the value of gt_{int} , $gt_{int} = \pi/\sqrt{2}$, in the Fig. 1 is a small value for a trapping state. In the Fig. 10 we choose $\bar{n} = 0$ (zero temperature) and $gt_{int} = \pi/2$ radians. This is a trapping state with photon number $n = 3$ also a small value. The behaviors in Fig. 10 are qualitatively the same as in the Fig. 1. In the Fig. 11 the temperature is increased so that $\bar{n} = 0.1$. The qualitative change compared with Fig. 10 follows the qualitative change between Fig. 1 (zero temperature) and Fig. 2 (finite temperature).

For the Fig. 12 we choose $gt_{int} = \pi/\sqrt{19}$ so that the trapping state photon number is increased to $n = 18$, larger than in Figs. 1 and 2 and 10 and 11. The Fig. 13 shows the same data for $\bar{n} = 0.1$; the change here is the emergence of the threshold for \tilde{Q}_e , \tilde{Q}_g just beyond $N_{ex} = 60$.

The Figs. 14 (a) and (b) plot the dependence of \tilde{Q}_g and \tilde{Q}_e respectively on the collection time t for $gt_{int} = \pi/\sqrt{2}$. The chosen t values are 1, 5, 10, 100, 1000 and ∞ times the cavity damping time and the plots are given as functions of N_{ex} . These results compare with the Fig. 5 in [42] evaluated for $gt_{int} = 1.54$ and plotted as a function of collection time t . Finally the Figs. 15 (a) and (b) plot the dependence of Q_g and Q_e respectively on N the fixed number of atoms collected as a function of N for $gt_{int} = 1.54$ and $\bar{n} = 0.1$. The chosen N values are 20, 50, 100, 500, 1000, and ∞ .

The reason for the differences in the atomic Q -functions in the limit of a large number of atoms and that in the limit of long time for $N_{ex} \ll 1$ can be easily seen. These limits correspond to high cavity damping or a low rate of injection of the atoms. In either case the cavity field decays to a state of thermal equilibrium during the time interval between the arrival of two successive atoms into the cavity. Hence each atom sees the same field, i.e. the thermal field, on its entry into the cavity. The probability of an atom exiting the cavity in a given state is, therefore, the same for every atom. In other words, there is no correlation between the states of two atoms exiting from the cavity and so the probability that an atom exits in a given state follows a binomial distribution. Let β_g be the probability that an atom exits from the cavity in its ground state. If one observes groups of a fixed number N of atoms exiting from the cavity then the number N_g of atoms detected in the ground state is governed by a binomial distribution for which the probability of success is β_g . Hence

$$\langle N_g \rangle = N\beta_g, \quad \langle N_g(N_g - 1) \rangle = N(N - 1)\beta_g^2. \quad (4.1)$$

As a consequence of (4.1) it follows that $Q_g = -\beta_g$. The same relations hold for the Q -function Q_e for the upper state with β_g replaced by $1 - \beta_g$. For the exactly solvable case of the micromaser discussed above, $\beta_g = \sin^2(\pi/\sqrt{2}) \approx 0.36$. Hence Q_g and Q_e in this case are predicted to be approximately -0.64 and -0.36 re-

spectively for N_{ex} close to zero. This is in agreement with the plots presented in Figs. 1.

If, on the other hand, one observes the groups of atoms for a fixed time interval t then the number N of atoms entering the cavity in that interval is governed by the pumping statistics. The expressions corresponding to (4.1) in this case are obtained by averaging (4.1) over the number N of atoms. Now, the pumping statistics has been assumed to be a binomial distribution for which the probability of success is p . Hence $\langle N \rangle = Rt$ and $\langle N^2 \rangle - \langle N \rangle^2 = Rt(Rt - p)$. On averaging (4.1) over N we get

$$\langle N_g \rangle = Rt\beta_g, \quad \langle N_g(N_g - 1) \rangle = Rt(Rt - p)\beta_g^2. \quad (4.2)$$

As a result, $\tilde{Q}_g = -p\beta_g$. The same arguments hold for \tilde{Q}_e with β_g replaced by $1 - \beta_g$. In particular, for the Poisson pumping $p = 0$, it is expected that $\tilde{Q}_g = \tilde{Q}_e = 0$ for N_{ex} close to zero. This is clearly in agreement with the plots presented above.

As N_{ex} increases, the correlations between the successive atoms start dominating. In particular for $N_{ex} \rightarrow \infty$, i.e., in the limit of an ideal cavity, the steady state of the cavity field approaches a trapping state and all the atoms exit in the excited state which is the state in which they enter the cavity. Hence, in this case, it is expected that $Q_e \rightarrow -1$, $\tilde{Q}_e \rightarrow -p$, $Q_g \rightarrow \tilde{Q}_g \rightarrow 0$. With the exception of \tilde{Q}_e whose asymptotic, large N_{ex} behavior could not actually be shown in the figures this behavior is borne out by the figures presented above.

ACKNOWLEDGMENTS

RRP gratefully acknowledges enlightening discussions with Dr. B.-G. Englert and Prof. H. Walther. Both RRP and SAK are grateful to the UK's EPSRC for the financial support which has enabled this work to be carried out.

APPENDIX A:

In this Appendix we outline a method for evaluating the Q -functions given by (3.21) and (3.23). Note that those two Q -parameters can be written as

$$Q = \frac{2\eta_g}{Tr_f[F_g\rho_{ss}]} Tr_f \left[F_g \left(1 - \frac{1 - (AB)^K}{K(1 - AB)} \right) \times \left(\frac{1}{(1 - AB)} \right) A F_g \rho_{ss} \right] - \eta_g K Tr_f[F_g\rho_{ss}], \quad (A1)$$

where $K = N$, $A = \Lambda_p$, $B = F_0$ for $Q = Q_g$ and $K = Rt$, $A = \tilde{\Lambda}_p$, $B = \tilde{F}_0$ for $Q = \tilde{Q}_g$.

To evaluate (A1), it is convenient to work in the eigenrepresentation of the operator AB . Let $\{\rho_i\}$ and $\{\tilde{\rho}_i\}$ be

the right and left eigenfunctions of AB corresponding to the eigenvalues $\{\lambda_i\}$, i.e.,

$$AB\rho_i = \lambda_i\rho_i, \quad \tilde{\rho}_i AB = \lambda_i\tilde{\rho}_i. \quad (\text{A2})$$

We assume that the eigenvalue $\lambda_0 = 1$, i.e., ρ_0 is the steady state density matrix of the micromaser ($\rho_{ss} = \rho_0$).

On taking the trace on both sides of the first of the equations in (A2) and on using the trace conserving property of A and B , i.e., the relations $Tr(A\rho) = Tr(\rho)$, $Tr(B\rho) = Tr(\rho)$, which are a consequence of the identification of A and B with the operators Λ_p , $\tilde{\Lambda}_p$, F_0 , \tilde{F}_0 and the trace conserving property (3.19), it follows that $Tr(\rho_i) = \lambda_i Tr(\rho_i)$, and since λ_0 is the only eigenvalue assumed to be unity, this leads to the result

$$Tr(\rho_i) = 0, \quad \text{if } i \neq 0. \quad (\text{A3})$$

Now, the eigenstates $\{\rho_i\}$ and $\{\tilde{\rho}_i\}$ are orthogonal with respect to the trace as a scalar product. Let us assume that they are orthonormalized so that

$$Tr(\tilde{\rho}_i\rho_j) = \delta_{ij}. \quad (\text{A4})$$

As a consequence of (A4), we can write

$$AB(\rho_i) = \sum_j C_{ij}^g(\rho_j), \quad (\text{A5})$$

where

$$C_{ij}^g = Tr(\tilde{\rho}_j AB\rho_i). \quad (\text{A6})$$

Now we can express the averages and the Q -functions in terms of the eigenstates of AB using (A6).

Since $Tr(AF_g\rho) = Tr(F_g\rho)$, it follows on using (A5) that

$$Tr(F_g\rho) = C_{00}^g. \quad (\text{A7})$$

In the same way, it can be shown that the expression (A1) for Q reduces to

$$Q = -p\eta_g C_{00}^g + \frac{2\eta_g}{C_{00}^g K} \sum_{i \neq 0} \left[\frac{C_{i0}^g C_{0i}^g}{(1-\lambda_i)^2} \left((1-\lambda_i)K - 1 \right) + [1 - p(1-\lambda_i)]^K \right]. \quad (\text{A8})$$

The Q -functions can thus be computed by evaluating the right and the left eigenstates and eigenvalues of the operator AB , where A and B are defined after (A1).

[†] Currently at The Institute of Mathematical Sciences, C.I.T. Campus, Taramani, Chennai - 600 113, India. E-mail: arun@imsc.ernet.in

[‡] E-mail: robin.bullough@umist.ac.uk

- [1] P. Filipowicz, J. Javanainen, and P. Meystre, Phys. Rev. **A34**, 3077 (1986).
- [2] L. Davidovich, J.M. Raimond, M. Brune, and S. Haroche, Phys. Rev. **A36**, 3771 (1987).
- [3] J. Bergou, L. Davidovich, M. Orszag, C. Benkert, M. Hillery, and M.O. Scully, Phys. Rev. **A40**, 5073 (1989).
- [4] P. Meystre, G. Rempe, and H. Walther, Opt. Lett. **13**, 1078 (1988).
- [5] L. Davidovich, S.Y. Zhu, A.Z. Khoury, and C. Su, Phys. Rev. **A46**, 1630 (1992).
- [6] S.Y. Zhu, M.S. Zubairy, C. Su, and J. Bergou, Phys. Rev. **A45**, 499 (1992).
- [7] F.L. Kien, G.M. Meyer, M.O. Scully, H. Walther, and S.Y. Zhu, Phys. Rev. **A49**, 1367 (1994).
- [8] J. Bergou and M. Hillery, Phys. Rev. **A49**, 1214 (1994).
- [9] R.R. Puri, C.K. Law, and J.H. Eberly, Phys. Rev. **A50**, 4212 (1994); C.K. Law, R.R. Puri, and J.H. Eberly, Appl. Phys. **B60**, S11 (1995).
- [10] A. Joshi, A. Kremid, N. Nayak, B.V. Thompson, and R.K. Bullough, J. Mod. Opt. **43**, 971 (1996).
- [11] R.K. Bullough *et al.*, in *Notions and Perspectives of Nonlinear Optics*, Series in Nonlinear Optics Vol. 3, edited by O. Keller (World Scientific Publ. Co. Ltd.: Singapore, 1996) p. 10 and references. Additional typescript 'Acknowledgements, Notes and Corrections', available from R.K. Bullough.
- [12] A. Joshi, A. Kremid, N. Nayak, B.V. Thompson, and R.K. Bullough, in *ICONO '95: Atomic and Quantum Optics: High Precision Measurements* edited by N. Bagayev and Anatoly S. Chirkin (Proc. SPIE 2799, Washington, 1996) p. 35.
- [13] R.R. Puri, F. Haake, and D. Forster, J. Opt. Soc. Am. **13**, 2689 (1996).
- [14] H. Walther, Phys. Rep. **219**, 263 (1992).
- [15] E.T. Jaynes and F.W. Cummings, Proc. IEEE **51**, 89 (1963).
- [16] M. Tavis and F.W. Cummings, Phys. Rev. **170**, 379 (1968).
- [17] N.M. Bogoliubov, R.K. Bullough, and J. Timonen, J. Phys. A: Math. Gen. **29**, 6305 (1996).
- [18] For extension of the q-bosons to the Maxwell-Bloch systems and other integrable (solvable) quantum models see N.M. Bogoliubov, A.V. Rybin, R.K. Bullough, and J. Timonen, Phys. Rev. **A 52**, 1487 (1995).
- [19] R.K. Bullough and R.R. Puri, in Proceedings of the International Conference on 'Nonlinear Dynamics: Integrability and Chaos', edited by M. Daniel (World Scientific Publ. Co. Ltd.: Singapore, 1998), to appear. Also see R.K. Bullough, N.M. Bogoliubov, and R.R. Puri, 'Quantum integrability and quantum chaos in the micromaser', to appear in the Russian Journal of Theoretical and Mathematical Physics.
- [20] G. Rempe, F. Schmidt-Kaler, and H. Walther, Phys. Rev. Lett. **64**, 2783 (1990).
- [21] G. Rempe and H. Walther, Phys. Rev. **A42**, 1650 (1990).

* Permanent Address: Theoretical Physics Division, Central Complex, Bhabha Atomic Research Centre, Mumbai - 400 085, India. E-mail: rrpuri@apsara.barc.ernet.in

- [22] M. Brune, J.M. Raimond, P. Goy, L. Davidovich, and S. Haroche, Phys. Rev. Lett. **59**, 1899 (1987).
- [23] R.K. Bullough, N. Nayak, and B.V. Thompson, in *Recent Developments in Quantum Optics*, edited by R. Inguva (Plenum Press, New York, 1993).
- [24] L.A. Lugiato, M.O. Scully, and H. Walther, Phys. Rev. **A 36**, 740 (1987).
- [25] C. Wagner, R.J. Brecha, A. Schenzle, and H. Walther, Phys. Rev. **A47**, 5068 (1993).
- [26] H.-J. Briegel, B.-G. Englert, N. Sterpi, and H. Walther, Phys. Rev. **A49**, 2962 (1994).
- [27] U. Herzog, Phys. Rev. **A50**, 783 (1994).
- [28] H. Paul and Th. Richter, Opt. Commun. **85**, 508 (1991).
- [29] B.-G. Englert, N. Sterpi, and H. Walther, Opt. Commun. **100**, 526 (1993).
- [30] We are indebted to B.-G. Englert for first pointing out to us the exact equivalence between ‘coarse-graining’ and the choice of a continuous time Poisson distribution for the pumping of the atoms. We confirm this exact equivalence at both fixed N and fixed t in this paper.
- [31] L. Mandel, Opt. Lett. **4**, 205 (1979).
- [32] H.-J. Briegel and B.-G. Englert, Phys. Rev. **A47**, 3311 (1993).
- [33] N. Nayak, Opt. Commun. **118**, 114 (1995).
- [34] N. Nayak, A. Kremid, B.V. Thompson, and R.K. Bullough, in *Quantum Communication and Measurement*, edited by V.P. Belavkin, O. Hirota, and R.L. Hudson (Plenum Press: New York, 1995), p. 521.
- [35] S. Sachdev, Phys. Rev. **29**, 2627 (1984).
- [36] G. Lindblad, Commun. Math. Phys. **48**, 119 (1976).
- [37] J. Krause, M.O. Scully, and H. Walther, Phys. Rev. **A 36**, 4547 (1987).
- [38] It is wholly natural, and manipulatively convenient in the present context as well, to introduce just such a concept, the ‘conditional density matrix’ (or ‘conditional density operator’). The properties of this object are naturally defined by analogy with the corresponding probability density (probability measure), and Eq. (2.11), (2.12), (2.13) in particular are examples of such natural definitions. The steps at (2.16) and (2.17) to (2.18) and then (2.19), with especially (2.17) defining joint and conditional probabilities in their usual way, shows how natural this idea of conditional density operators actually is. Evidently (2.19) is finally a correct result, and the other definitions (of conditional density operators) invoked serve only to reach this result in a manipulatively convenient way. We believe these ideas have been invoked by a number of different workers but cannot give an explicit reference.
- [39] Recall $t_{i+1} - t_i$ is stochastic in practice: in [20] for example, $Rt_{int} \sim 1/200$.
- [40] A. Joshi and R.K. Bullough, to be published.
- [41] P. Filipowicz, J. Javanainen, and P. Meystre, J. Opt. Soc. Am. **B3**, 906 (1986).
- [42] O. Benson, M. Weidinger, G. Raithel, and H. Walther, J. Mod. Opt. **44**, 2011 (1997).
- [43] On the computer each value of gt_{int} which is achievable, namely a finite decimal number, defines a trapping state. But such trapping states may require photon numbers n very different from the n 's considered.

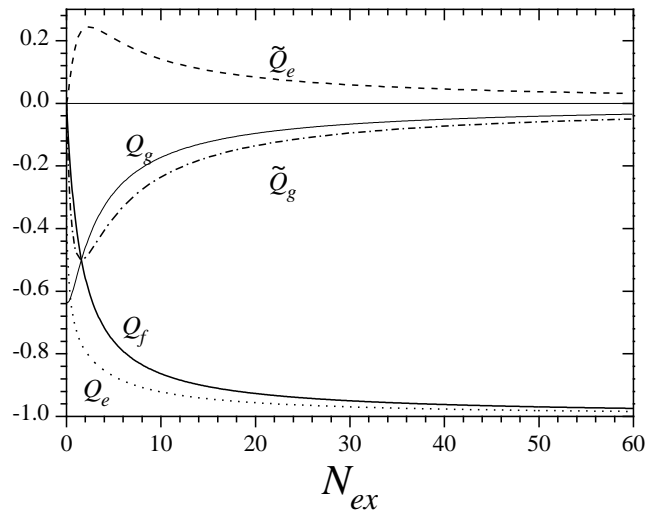


FIG. 1. The Q -parameters, Q_g , Q_e , \tilde{Q}_g , \tilde{Q}_e , and Q_f as functions of N_{ex} for $gt_{int} = \pi/\sqrt{2}$, $\bar{n} = 0$ and for Poissonian pumping of the excited atoms into the cavity ($p = 0$). Q_f is multiplied by 0.1 in order to compare it with the atomic Q -parameters.

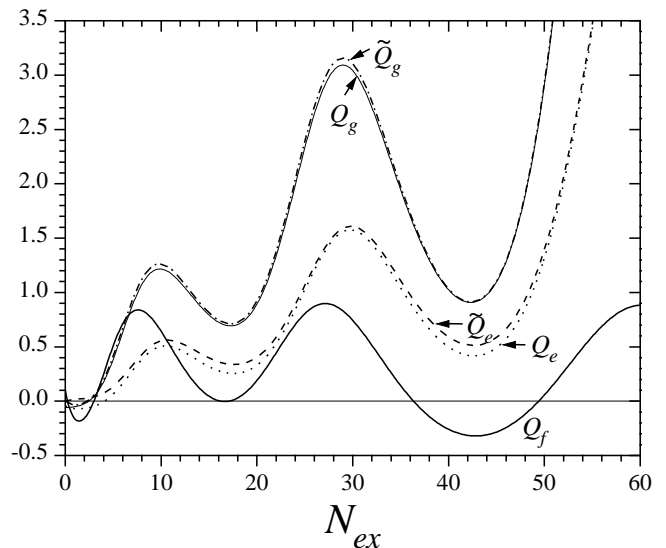


FIG. 2. The same as Fig. 1, but for non-zero thermal photons ($\bar{n} = 0.1$).

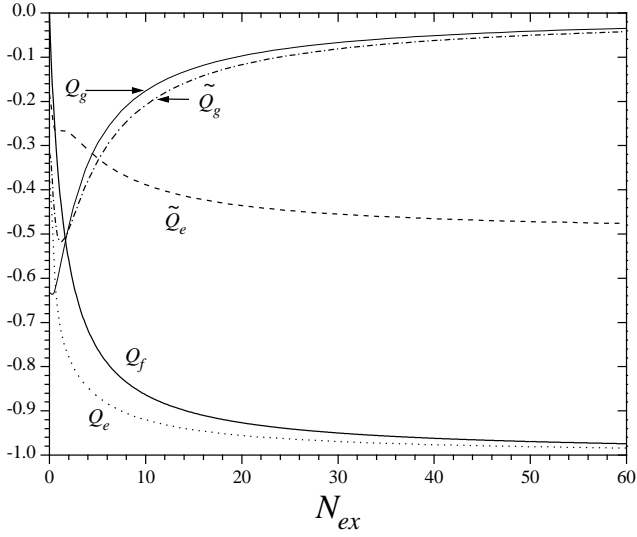


FIG. 3. The same as Fig. 1, but for binomial pumping of the excited atoms into the cavity with excitation probability, $p = 0.5$ (deviation from Poissonian pumping).

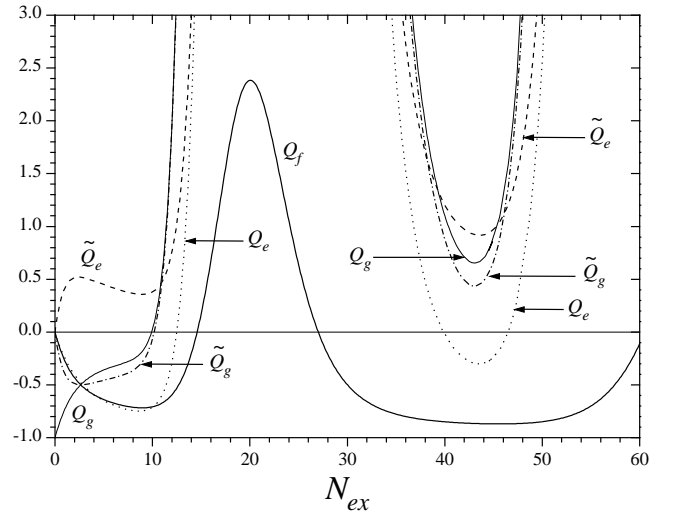


FIG. 5. The same as Fig. 4, but for $\bar{n} = 0$.

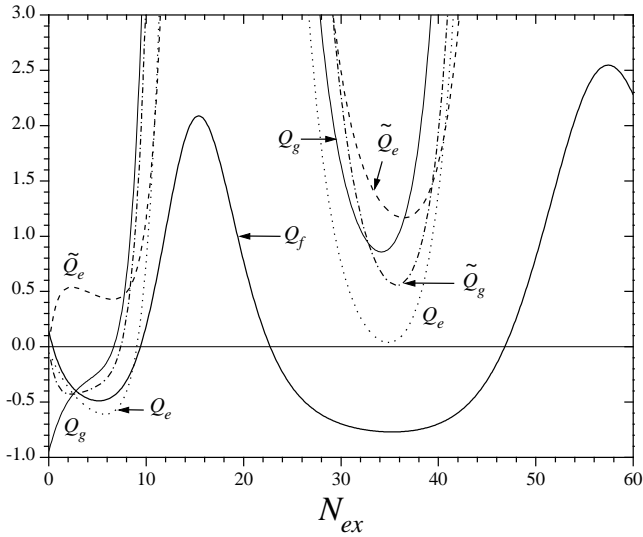


FIG. 4. The Q -parameters, Q_g , Q_e , \tilde{Q}_g , \tilde{Q}_e , and Q_f as functions of N_{ex} for $gt_{int} = 1.54$ and $\bar{n} = 0.145$ and for Poissonian pumping of the excited atoms into the cavity ($p = 0$). These parameters correspond to the Fig. 3 of [20].

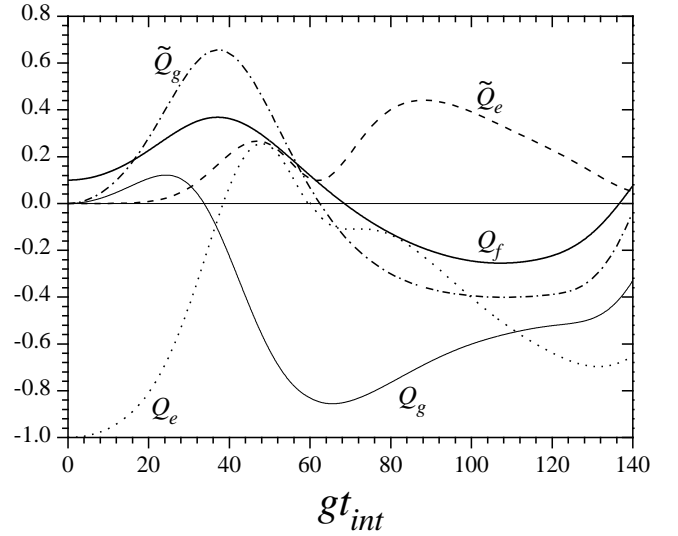


FIG. 6. The Q -parameters, Q_g , Q_e , \tilde{Q}_g , \tilde{Q}_e , and Q_f as functions of gt_{int} when $\bar{n} = 0.1$ and $N_{ex} = 1$ for the case of Poissonian pumping of the excited atoms.

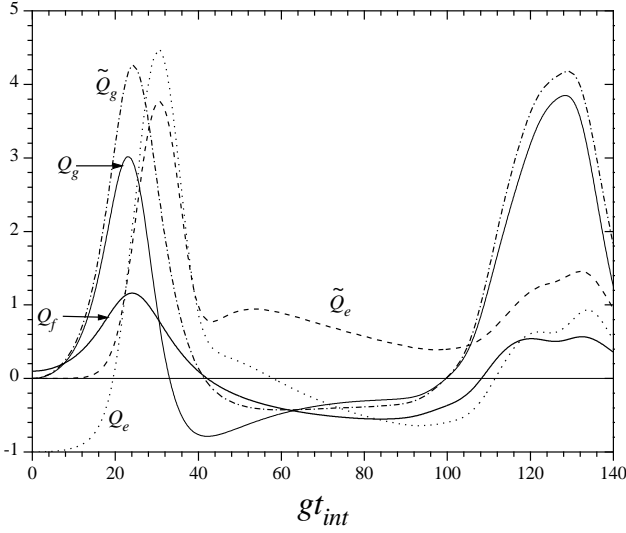


FIG. 7. The Q -parameters, Q_g , Q_e , \tilde{Q}_g , \tilde{Q}_e , and Q_f as functions of gt_{int} when $\bar{n} = 0.1$ and $N_{ex} = 5$ for the case of Poissonian pumping of the excited atoms.

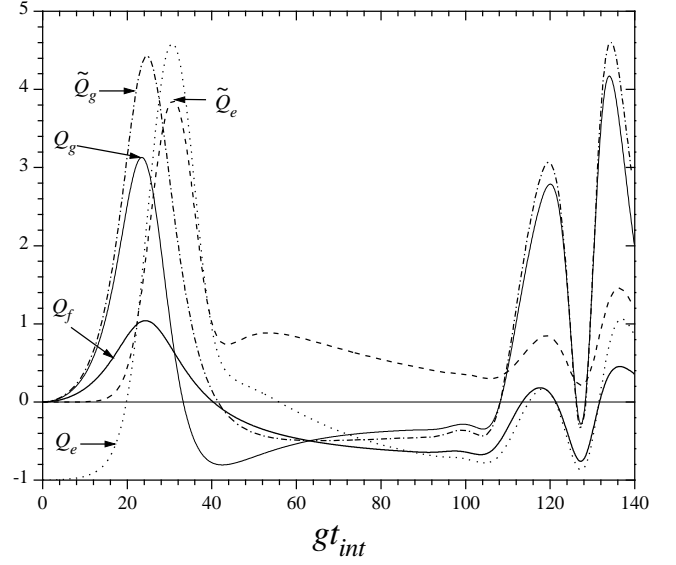


FIG. 9. The same as Fig. 7 but with $\bar{n} = 0$.

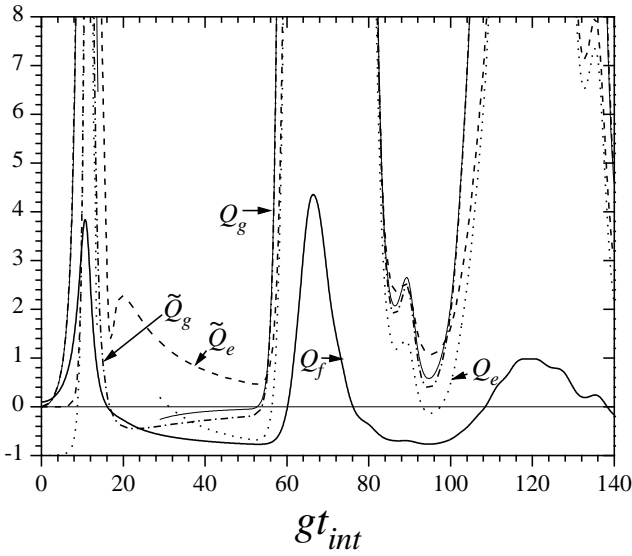


FIG. 8. The same as Figs. 6 and 7, but for $N_{ex} = 30$. Computational difficulties have prevented us following Q_e for $17 \lesssim gt_{int} \lesssim 30$.

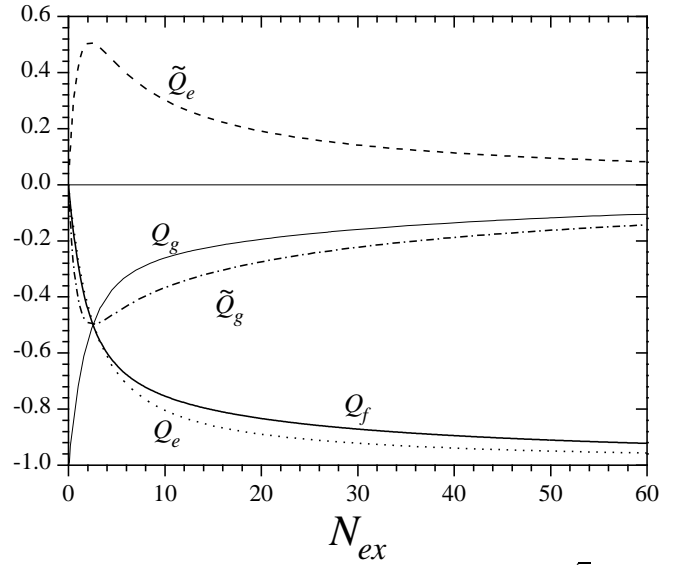


FIG. 10. The same as Fig. 1 but for $gt_{int} = \pi/\sqrt{4} = \pi/2$ and $\bar{n} = 0$.

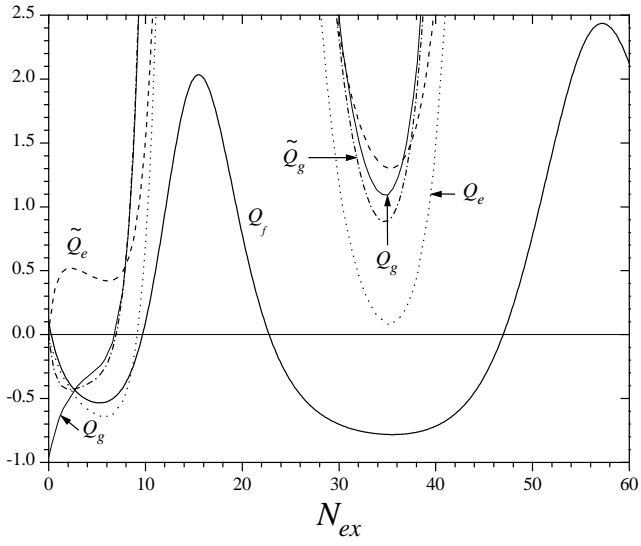


FIG. 11. The same as Fig. 10 but for finite temperature ($\bar{n} = 0.1$).

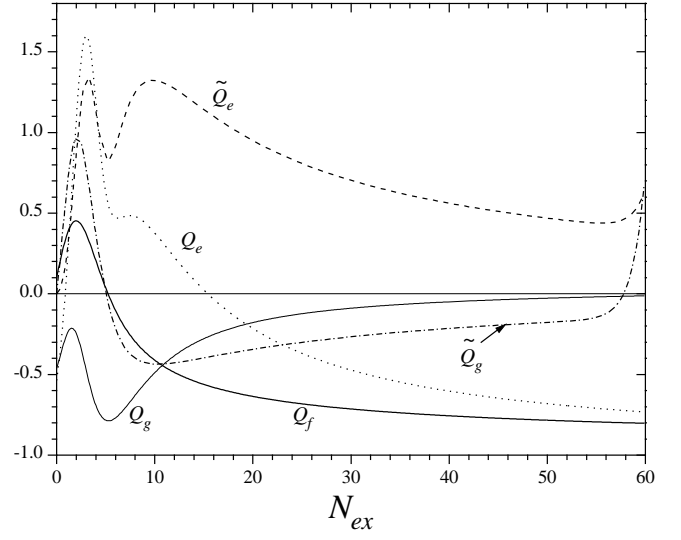


FIG. 13. The same as Fig. 12 but for finite temperature ($\bar{n} = 0.1$).

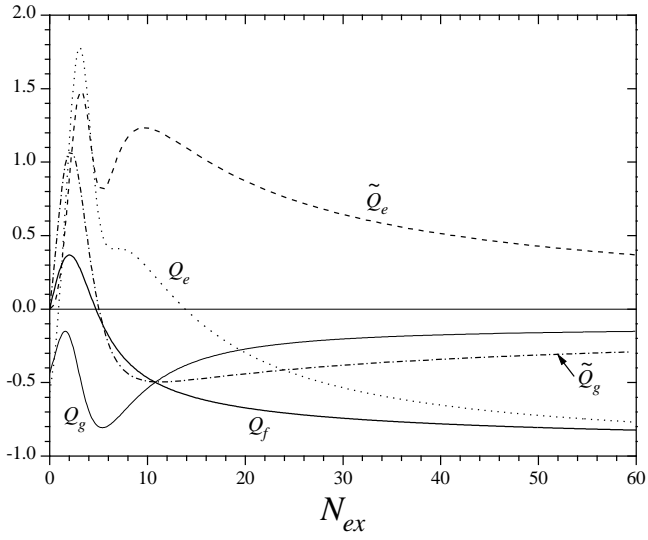


FIG. 12. The same as Fig. 1 but for $gt_{int} = \pi/\sqrt{19}$ and $\bar{n} = 0$.

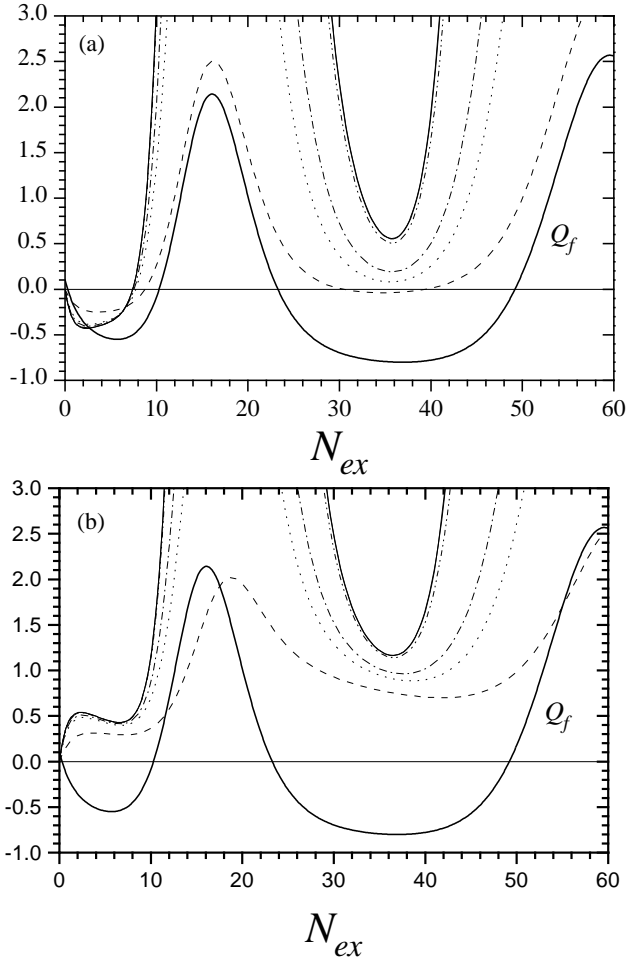


FIG. 14. The dependence of (a) \tilde{Q}_g and (b) \tilde{Q}_e on the collection time t for $gt_{int} = 1.54$ and $\bar{n} = 0.1$. The t values are 1 (---), 5 (···), 10 (-·-), 100 (-·-·-), 1000 (- - -), and ∞ (—).

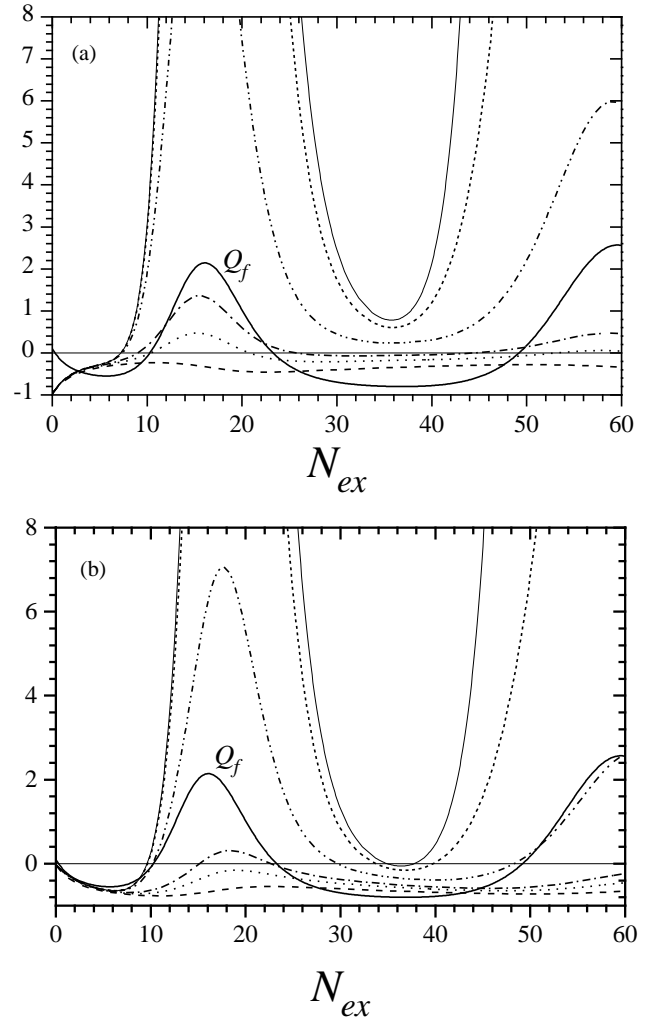


FIG. 15. The dependence of (a) Q_g and (b) Q_e on the number of atoms collected, N for $gt_{int} = 1.54$ and $\bar{n} = 0.1$. The N values are 20 (---), 50 (···), 100 (-·-), 500 (- - -), 1000 (- · -), and ∞ (—).